DOI: 10.1002/chem.201101832

Design and Photophysical Properties of Zinc(II) Porphyrin-Containing Dendrons Linked to a Central Artificial Special Pair

Frédérique Brégier,[a] Shawkat M. Aly,[b, c] Claude P. Gros,*[a] Jean-Michel Barbe,[a] Yoann Rousselin,[a] and Pierre D. Harvey*[a, b]

Abstract: The click chemistry synthesis and photophysical properties, notably photo-induced energy and electron transfers between the central core and the peripheral chromophores of a series of artificial special pair–dendron systems (dendron = **G1**, **G2**, **G3**; **G*x*** = zinc(II) tetra-*meso*-arylporphyrin-containing polyimides) built upon a central core of dimethylxanthenebis(metal(II) porphyrin) (metal = zinc, copper), are reported. The dendrons act as singlet and triplet energy acceptors or donors, depending on the dendrimeric systems. The presence of the paramagnetic d^9 copper(II) in the dendrimers promotes singlet–triplet energy transfer from the zinc(II) tetra-*meso*-arylporphyrin to the bis(copper(II) porphyrin) unit and slow triplet–triplet energy transfer from the central bis(copper(II) porphyrin) fragment to the peripheral zinc(II) tetra-*meso*-arylporphyrin. If bis(zinc(II) porphyrin) is the central core, evidence for chain folding is observed; this is unambiguously demonstrated by the presence of triplet–triplet energy transfer in the heterobimetallic systems, a process that can only occur at short distances.

Keywords: click chemistry · dendrimers · electron transfer · energy transfer · fluorescence · phosphorescence · porphyrinoids

Introduction

Porphyrin-containing dendrimers have been the subject of intense investigations during the past decade or so,[1] and an important review on the subject was recently written by Li and Aida.[2] A main reason for such interest is that these systems represent good models for the light-harvesting devices of Photosystems I and II in plants and cyanobacteria.[3] In previously reported model systems, the core of the dendrimers may or may not contain a chromophore or redox-active center, and evidence for antenna and electron transfer process effects similar to those observed in Nature were noted. Except for one earlier example,[3b] all these systems lacked a key element, that is, the central special pair. This entity appears in Nature because the structural flexibility (relative orientation and intermolecular distance) allows modulation of the redox potential and the position of the Soret and Q bands in the visible spectrum.[3] Less obviously, placing two chromophores very close together has the effect of increasing the bandwidth of their absorption and emission spectra.[4] Consequently, for singlet energy transfer processes operating according to the coulombic Förster theory,[5] the *J* integral (i.e., the spectral overlap between the lowest energy absorption band of the energy acceptor and the fluorescence one of the donor) is larger and, therefore, the rate is faster. To design molecular models that resemble the special pair–antenna assemblies of photosystems more closely, it now becomes appropriate to couple an artificial pair with dendrimeric antennas and investigate their photophysical properties along with the energy transfer processes from the surrounding antenna molecules to the central artificial special pair. Herein, we report the syntheses and complex photophysical behavior of a series of artificial pair–dendrons (dendron = **G1**, **G2**, **G3**) built upon a dimethylxanthenebis(metal(II) porphyrin) (metal = zinc or copper) as the central core and artificial special pair (Scheme 1). A zinc(II) tetra-*meso*-arylporphyrin unit is attached to the dendrons and acts as a singlet and triplet energy acceptor or donor, depending on the dendrimeric systems. The presence of the paramagnetic d^9 copper(II) unit in the dendrimers promotes both singlet–triplet energy transfer from the zinc(II) tetra-*meso*-arylporphyrin to the bis(copper(II) porphyrin) chro-

[a] Dr. F. Brégier, Prof. C. P. Gros, Dr. J.-M. Barbe, Dr. Y. Rousselin, Prof. P. D. Harvey
Université de Bourgogne, ICMUB (UMR 5260)
9 Avenue Alain Savary, BP 47870
21078 Dijon Cedex (France)
Fax.: (+33) 380-396-117
E-mail: Claude.Gros@u-bourgogne.fr

[b] S. M. Aly, Prof. P. D. Harvey
Département de Chimie, Université de Sherbrooke
Sherbrooke, Québec, Canada J1K 2R1
Fax: (+1) 819-821-8017
E-mail: Pierre.Harvey@USherbrooke.ca

[c] S. M. Aly
On leave from:
Chemistry Department, Faculty of Science
Assiut University, Assiut (Egypt)

Supporting information for this article is available on the WWW under http://dx.doi.org/10.1002/chem.201101832, and contains a CIF file giving X-ray structural data of **8**; ^{1}H and ^{13}C NMR spectra (Figures SI1–SI20); mass spectra (Figures SI21–SI39); EPR spectra of compounds **33**, **34**, and **35** (Figures SI40–SI42); emission, excitation, and absorption spectra (Figure SI43–SI48); transient absorption (Figure SI49); and computer modeling (for **34** and **35**, Figure SI50).

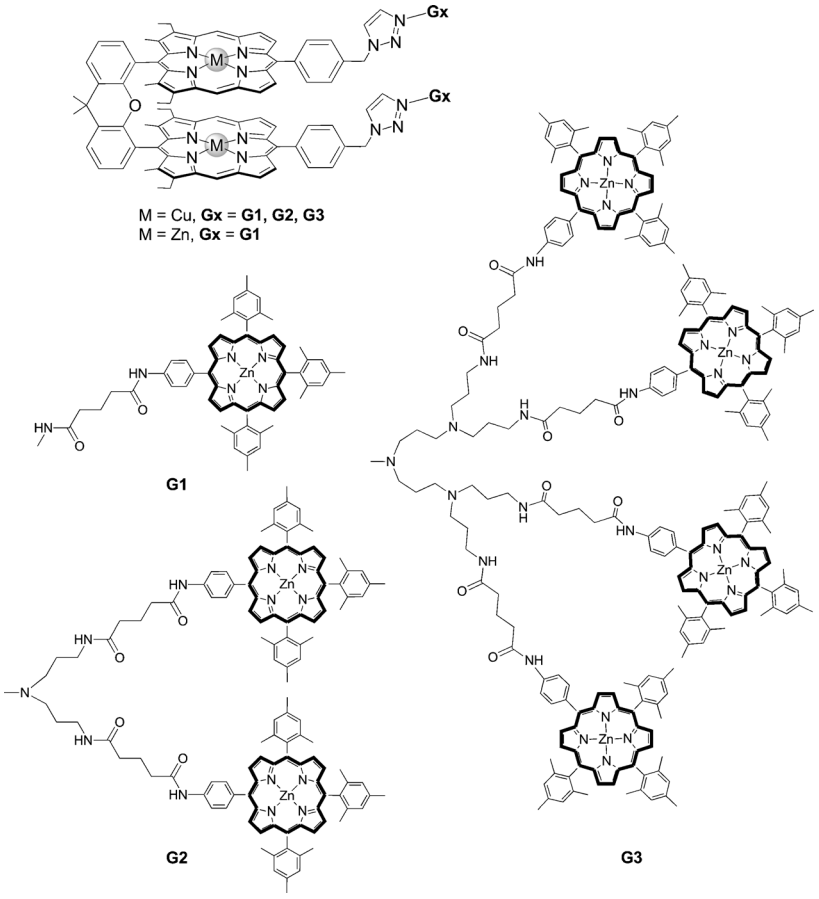

Scheme 1. Structures of the synthesized artificial pair-dendrons **G1**, **G2**, and **G3**.

mophore and triplet–triplet energy transfer from central bis(copper(II) porphyrin) fragment to the peripheral zinc(II) tetra-*meso*-arylporphyrins. If bis(zinc(II) porphyrin) is the central core, evidence for chain folding is observed. It is unambiguously demonstrated by the presence of triplet–triplet energy transfer, a process that can only occur at short distances.

Results and Discussion

The retrosynthetic pathway leading to the porphyrin dendrimers is shown in Scheme 2. The synthesis of the first-, second-, and third-generation dendrimers, covalently linked to a bisporphyrin unit, involves the preparation of a diazidoxanthene-bridged cofacial bisporphyrin as a key precursor. The standard convergent three-branch strategy was employed to give the disubstituted bisporphyrin derivative,[6] which can be easily prepared starting from dicarboxaldehyde-9,9-dimethylxanthene linker **1**, α-free ethyl ester pyrrole, and dipyrrylmethanedialdehyde **7**. Required α-free bisdipyrromethane **3** was prepared through a previously reported pathway.[6a] Dialdehyde bridge **1** was obtained by regioselective 4,5-dilithiation of 9,9-dimethylxanthene in the presence of dry DMF followed by hydrolysis of the intermediate imidate salt.[6a] Reaction of the 4,5-diformyl-9,9-dimethylxanthene **1** with 2-(ethoxycarbonyl)-3-ethyl-4-methylpyrrole in boiling ethanol afforded the corresponding ester-protected bis(dipyrryl)methane **2**. Subsequent saponification and decarboxylation proceeded smoothly to give α-free bisdipyrromethane **3** (86% yield).

Commercially available *para*-bromobenzonitrile was reduced with diisobutylaluminum hydride (DIBAL-H) in dry toluene, and acidic workup gave *para*-bromobenzyl aldehyde **4** (Scheme 3).[7] The bromine atom was subsequently replaced by an azide group by using sodium azide in DMSO.[8] Dipyrromethane **6** was obtained by a classical condensation of aldehyde **5** with excess neat pyrrole, catalyzed by trifluoroacetic acid (TFA; Scheme 3). A Vilsmeier formylation of **6** by using $POCl_3$/DMF followed by base hydrolysis gave dipyrrylmethane dialdehyde **7** in 48% yield.

The bisporphyrin was then obtained by direct condensation of **3** and **7** in the presence of *para*-toluenesulfonic acid (*p*-TsOH) followed by oxidation with *para*-chloranil (Scheme 4). After metalation by treatment with zinc acetate, resulting crude product **8** was purified by repeated column chromatography over silica gel. A very low yield (4%) was obtained for the final coupling step, in comparison with a

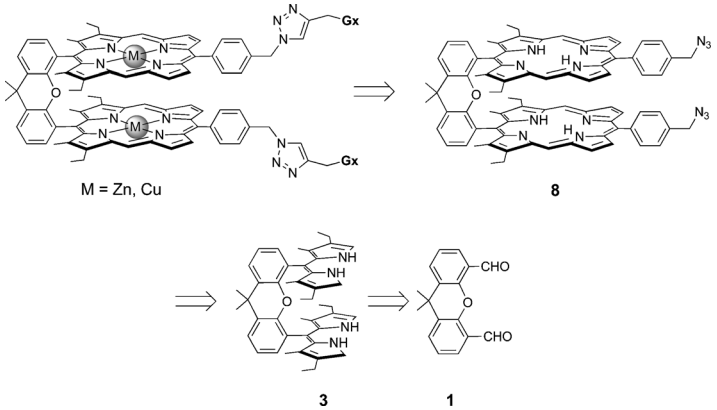

Scheme 2. Retrosynthetic analysis for the synthesis of the target compounds; see Scheme 1 for the structures of **Gx**.

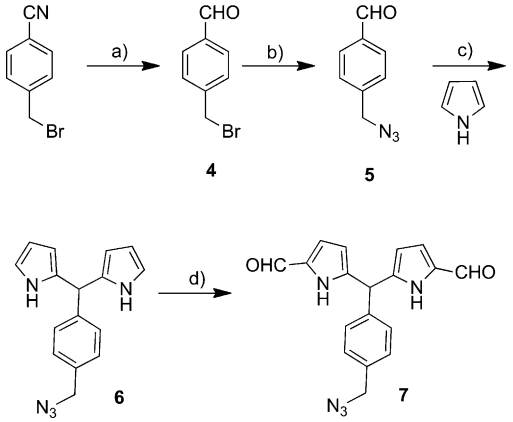

Scheme 3. Synthesis of dipyrrylmethanedialdehyde **7**. Reagents and conditions: a) DIBAL-H (1 M in CH_2Cl_2), dry toluene, 0 °C→RT, 3 h, then THF, HCl (1 M), 0 °C→RT, 1 h; b) NaN_3, DMSO, RT, 24 h, then H_2O; c) TFA, RT, 1 h; d) $POCl_3$, DMF, 0 °C→RT, 30 min, then **6**, DMF, 0 °C→RT→80 °C, 1 h, then saturated NaOAc, 80 °C, 20 min.

previously reported yield for the synthesis of a xanthene-bridged cofacial bisporphyrin (23 %).[6a]

The use of β-unsubstituted dipyrromethane was initially thought to be the cause of the low yield. However, exchange of dipyrromethane **7** with β-methyl-substituted dipyrromethane did not increase the yield for the synthesis of the bisporphyrin. Another explanation for the low yield could be the deactivation of the dipyrromethane by the benzyl azidomethyl group.

The zinc bisporphyrin can easily be demetalated by treatment with acid to form a green tetracation that was deprotonated with $NaHCO_3$ and washed with water to generate free-base bisporphyrin **9**. The chemical structures of **8** and **9** were confirmed by ^1H and ^{13}C NMR spectroscopy and MALDI-TOF mass spectrometry. Additionally, single crystals of **8** suitable for X-ray crystallographic characterization were obtained by slow diffusion of methanol into solution of the complex in dichloromethane. The resulting structure is shown in Figure 1a. This structure is very similar to that of previously reported $[Zn_2(DPX)]$ (DPX = 4,5-bis[5-(2,8,13,-17-tetraethyl-3,7,12,18-tetramethylporphyrinyl)]-9,9-dimethylxanthene).[6a] However, in our case, the distance between the two macrocycles is slightly smaller by 0.104 Å. Moreover, the interplanar angle between the two 24-atom cores is also smaller in **8** than in the crystal structure of $[Zn_2(DPX)]$. Selected structural data are summarized in Table 1. The mean plane separation is larger (0.113 Å) in compound **8** than in $[Zn_2(DPX)]$, whereas the Zn−Zn or Ct−Ct separation is smaller (d(Ct···Ct) was measured as the perpendicular distance from one macrocycle's 24-atom least-squares plane to the center of the 24-atom least-squares plane of the other macrocycle, see Table 1, footnote). This is due to the slightly domed shape of the two porphyrin rings. This shape results partly from the steric hindrance of phenyl groups placed at the *meso* position. Note that the ethyl groups in bisporphyrin **8** are oriented outward from the interplanar spacing, whereas one porphyrin in $[Zn_2(DPX)]$ has ethyl groups pointing in the opposite direction to the porphyrin plane. Figure 1b compares compound **8** (in black) and $[Zn_2(DPX)]$ (in gray).

The interplanar distance between the two macrocycles in **8** is 3.46 Å. This value is larger than that observed between the two (bacterio)chlorophylls in the bacterial special pair (3.2 Å), but slightly smaller than the value in Photosystem I (3.6 Å).[10] The Zn bisporphyrins of **8** stack in parallel layers, as usually observed in this type of compounds.[6a]

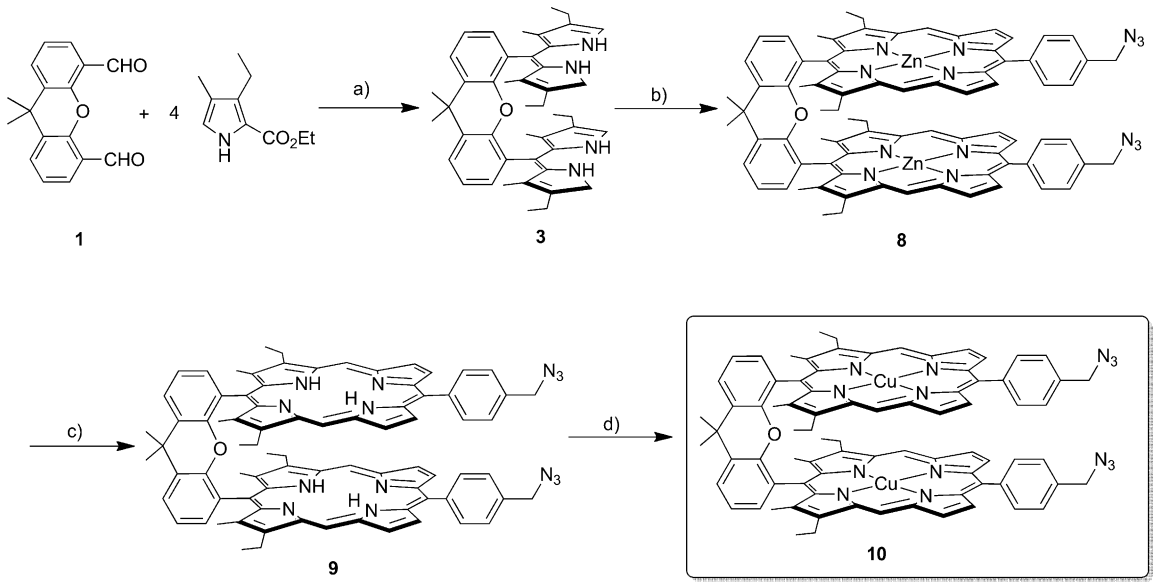

Scheme 4. Synthesis of the xanthene-bridged cofacial bisporphyrin. Reagents and conditions: a) EtOH, conc. HCl, reflux, 4 h, then NaOH, ethylene glycol, reflux, 3 h, 76 % over two steps; b) **7** (see Scheme 3), *p*-TsOH, methanol, then *para*-chloranil, then $Zn(OAc)_2{\cdot}H_2O$, $CHCl_3$/MeOH, 4.5 % over three steps; c) HCl (6 M), CH_2Cl_2, >99 %; d) $Cu(OAc)_2{\cdot}H_2O$, $NaOAc{\cdot}3H_2O$, $CHCl_3$/MeOH, 98 %.

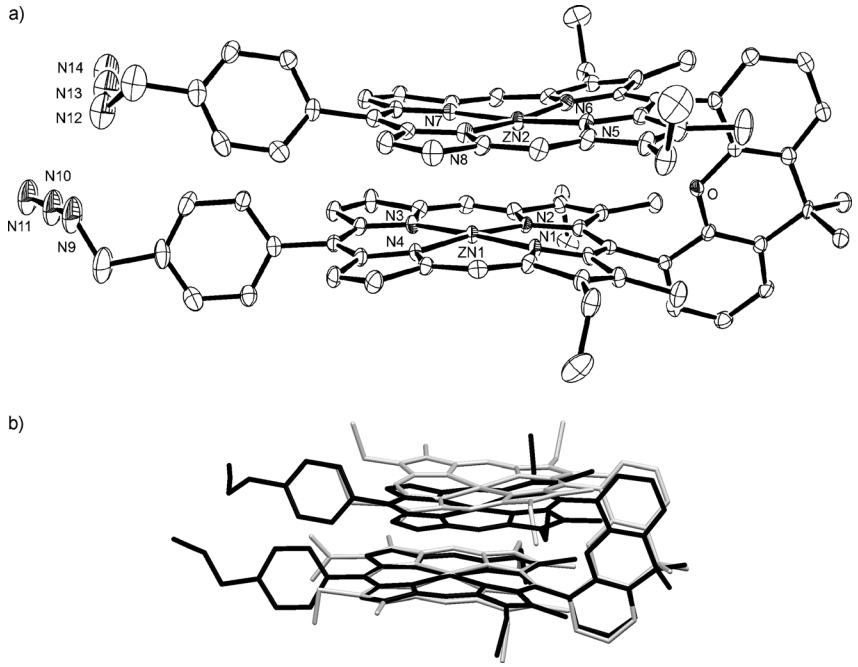

Figure 1. a) ORTEP[9] view of bisporphyrin **8**. Thermal ellipsoids are set at the 50% probability level, and hydrogen and disordered atoms have been omitted for clarity. b) Comparison of compound **8** (black) and [Zn_2(DPX)] (grey).

Table 1. Selected structural data for **8** and [Zn_2(DPX)].

	8	[Zn_2(DPX)][6a]
d(Zn···Zn) [Å]	3.6286(1)	3.7086(9)
Av. Zn···N_4 displacement [Å]	0.0801(5)	0.0917(3)
d(Ct···Ct)[a] [Å]	3.759	3.863
MPS[b] [Å]	3.811(6)	3.698(5)
Interplanar angle[c] [°]	3.11(3)	5.48(3)
Slip angle[d] [°]	28.20(2)	28.16
Lateral shift[e] [Å]	1.776	1.823

[a] Macrocyclic centers (Ct) were calculated as the centers of the four-nitrogen planes (N_4) for each macrocycle. [b] The plane separation was measured as the perpendicular distance from one macrocycle's 24-atom least-squares plane to the center of the 24-atom least-squares plane of the other macrocycle; the mean plane separation (MPS) is the average of the two plane separations. [c] The interplanar angles were measured as the angle between the two macrocyclic 24-atom least-squares planes. [d] The slip angles (α) were calculated as the average angle between the vector joining the two rings and the unit vectors normal to the two macrocyclic 24-atom least-squares planes ($\alpha=(\alpha_1+\alpha_2)/2$). [e] Lateral shift is defined as [$\sin(\alpha)\times$(Ct ··Ct)].[6a]

Biscopper(II) complex **10** was prepared in excellent yield (90%) by starting from **9** and using $Cu(OAc)_2{\cdot}2H_2O$ and potassium acetate in a methanol/chloroform mixture. Complex **10** gave satisfactory mass spectral analysis. Mesityl-substituted AB_3-porphyrin was chosen as the peripheral building block due to its favorable solubilizing properties and easy synthesis,[11] but this bulky group also prevents porphyrin aggregation and singlet–singlet annihilation (see below). The AB_3-porphyrin can be prepared through a MacDonald condensation of mesityldipyrromethane[12] with mesitaldehyde and 4-acetamidobenzaldehyde under Lindsey conditions (Scheme 5). Hydrolysis of porphyrin amide **11** with HCl/TFA at 80°C[11] gave porphyrin amine **12**, which was then acylated with glutaric anhydride to give compound **13** in quantitative yield. Activated ester **14** was prepared by condensation of this carboxylic acid derivative with *N*-hydroxysuccinimide in the presence of dicyclohexylcarbodiimide (DCC; $MeOCH_2$-CH_2OMe, 0–5°C, 18 h). Activated porphyrin ester **14** was isolated by column chromatography to remove any trace of unreacted acid porphyrin **13**. The synthesis of the poly(propylene imine) dendrimers is presented in Scheme 6. Precursor trimethylsilylpropynylamine[13] **15** was synthesized from commercially available *N*-[3-(trimethylsilyl)-2-propinyl]phthalimide by cleavage of the phthalimide group by hydrazine hydrate in ethanol. The second- and third-generation poly(propylene imine) dendrimers were prepared in a convergent manner from the commercially available bis(3-aminopropyl)amine commonly known as norspermidine. The primary amine functions were selectively protected by trifluoroacetyl groups by using standard reaction conditions[14] to give **16**, which was then reacted with propargyl bromide in the presence of sodium hydroxide in acetonitrile to give **17** in 55% yield (Scheme 6). The trifluoroacetamide groups were quantitatively cleaved with a methanolic aqueous ammonia solution to give **18**. The mono-Boc-protected norspermidine **20** was prepared from norspermidine via intermediates **16** and **19** by using a reported procedure (Scheme 6).[15] Tetra-alkylation with bromopropylphthalimide in the presence of potassium carbonate in acetonitrile at reflux gave tertiary amine **21**. The subsequent cleavage of the Boc group was carried out at 0°C with TFA in chloroform to give compound **22** in almost quantitative yield. The alkylation of the resulting secondary amine with 3-(trimethylsilyl)propargyl bromide[16] in the presence of potassium carbonate in acetonitrile gave compound **23** in 63% yield, then cleavage of the phthalimide groups by using hydrazine hydrate in ethanol finally gave **24** in quantitative yield. The chemical structure of poly(propylene imine) dendrimers was confirmed by ^1H and ^{13}C NMR spectroscopy and electrospray mass spectrometry.

The coupling of the active ester with the poly(propylene imine) dendrimers was carried out by using one molar equivalent of the activated ester for every primary amino end group present in the dendrimers. The reaction was performed in CH_2Cl_2 in the presence of *N*,*N*-diisopropylethylamine (DIPEA) at 20°C for 15 to 18 h to give compounds

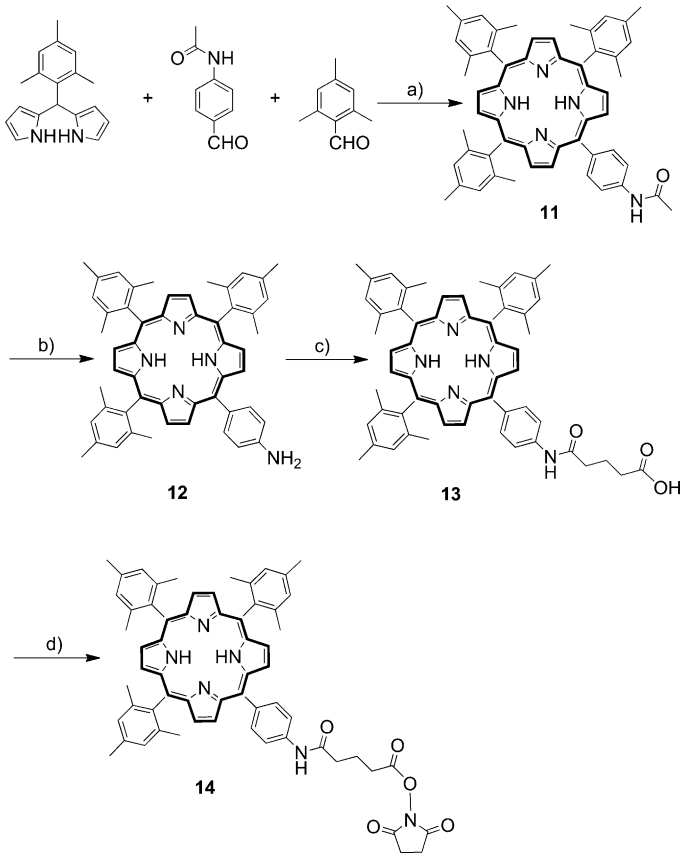

Scheme 5. Synthesis of the peripheral porphyrin. Reagents and conditions: a) $CHCl_3$, RT, 15 min, then $BF_3{\cdot}Et_2O$, $CHCl_3$, RT, 1 h, then 2,3-dichloro-5,6-dicyano-1,4-benzoquinone (DDQ), RT, 1 h, 10% over three steps; b) TFA, HCl (37%), 80°C, 19 h, 96%; c) glutaric anhydride, CH_2Cl_2, RT, 20 h, >99%; d) *N*-hydroxsuccinimide, DCC, $MeOCH_2CH_2OMe$, 0°C→RT, 18 h, 60%.

25, **26**, and **27** (Scheme 7). The protected first-generation (**G1**) dendron was isolated in 36% yield after chromatographic purification from acid-derived compound **13** generated during the reaction (Scheme 7), the second-generation (**G2**) dendron was separated by column chromatography on silica gel, and the third-generation **G3** dendron was isolated by recycling preparative size-exclusion chromatography (SEC) with CH_2Cl_2 as the eluent.

Cleavage of the trimethylsilyl group of **G1** was carried out at room temperature with tetrabutylammonium fluoride (TBAF) in CH_2Cl_2/THF (1:2) to give compound **28** (Scheme 8). **G1**, **G2**, and **G3** dendrons were easily metalated upon treatment with $Zn(OAc)_2{\cdot}2H_2O$ to give zinc complexes **29**, **30**, and **31**. All the dendrons were fully characterized by ^1H NMR spectroscopy and MALDI-TOF mass spectrometry. Finally, the Cu^I-catalyzed azide–alkyne 1,3-dipolar cycloaddition ("click") reaction[17] was used to connect the alkyne focal point poly(propylene imine) dendrons with the central core units through a convergent approach. The coupling of **8** with **29** was performed in CH_2Cl_2 in the presence of DIPEA and copper(I) iodide. The crude product was purified by column chromatography on silica gel to give the desired **G1** tetrazinc dendrimer **32** in 53% yield. The structure was confirmed by ^1H NMR spectroscopy and MALDI-TOF mass spectrometry. From the ^1H NMR spectra ($[D_8]$THF), the peaks of the methylene protons adjacent to the triazole carbon, the triazole proton, and the methylene protons adjacent to the nitrogen of triazole in **32** were found at $\delta = 4.82$, 8.26, and 6.17 ppm respectively.

Given the success of the synthesis of **32**, the coupling of **9** with **29** was realized under the same conditions. The MALDI-TOF MS analysis of the product showed a peak that was assigned to coupling compound **33** with two addi-

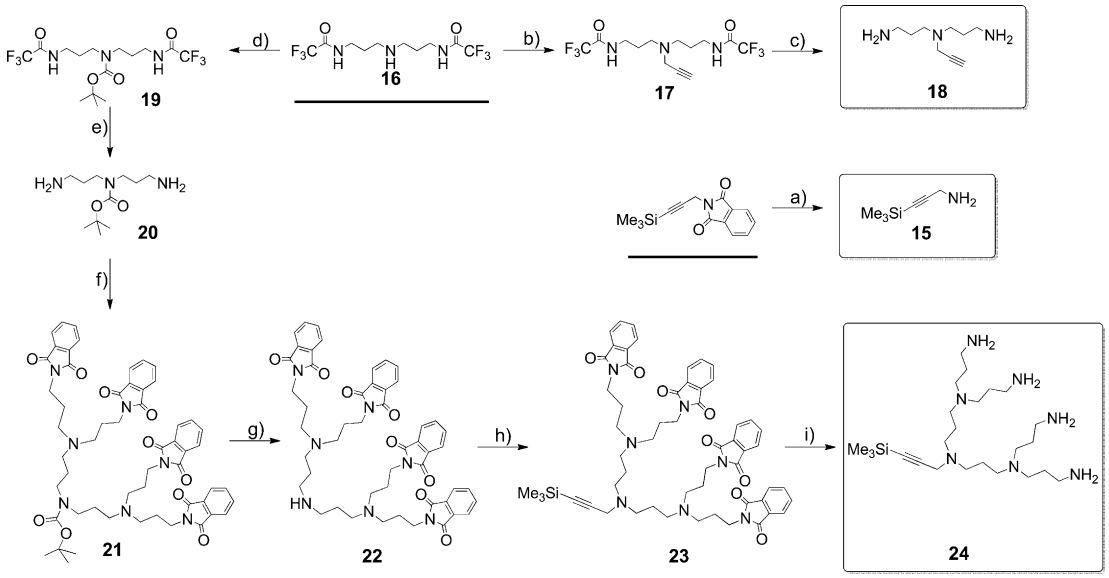

Scheme 6. Synthesis of the polypropylenimine dendrons. Reagents and conditions: a) $NH_2NH_2{\cdot}H_2O$, EtOH, 80°C, 2 h, >90%; b) KOH, $BrCH_2CCH$, CH_3CN, RT, 6 h, 55%; c) MeOH/25% NH_4OH (1:2), reflux, 20 h, >90%; d) Boc_2O, Et_3N, THF, RT, overnight, 59%; e) MeOH/NaOH (0.2 M; 1:1.1), RT, 20 h, >90%; f) *N*-(3-Bromopropyl)phthalimide, K_2CO_3, CH_3CN, reflux, 2 d, 69%; g) TFA, $CHCl_3$, 0°C, 4 h, >90%; h) K_2CO_3, $BrCH_2CCSiMe_3$, CH_3CN, 40°C, 18 h, 63%; i) $NH_2NH_2{\cdot}H_2O$, EtOH, 80°C, 2 h, >90%.

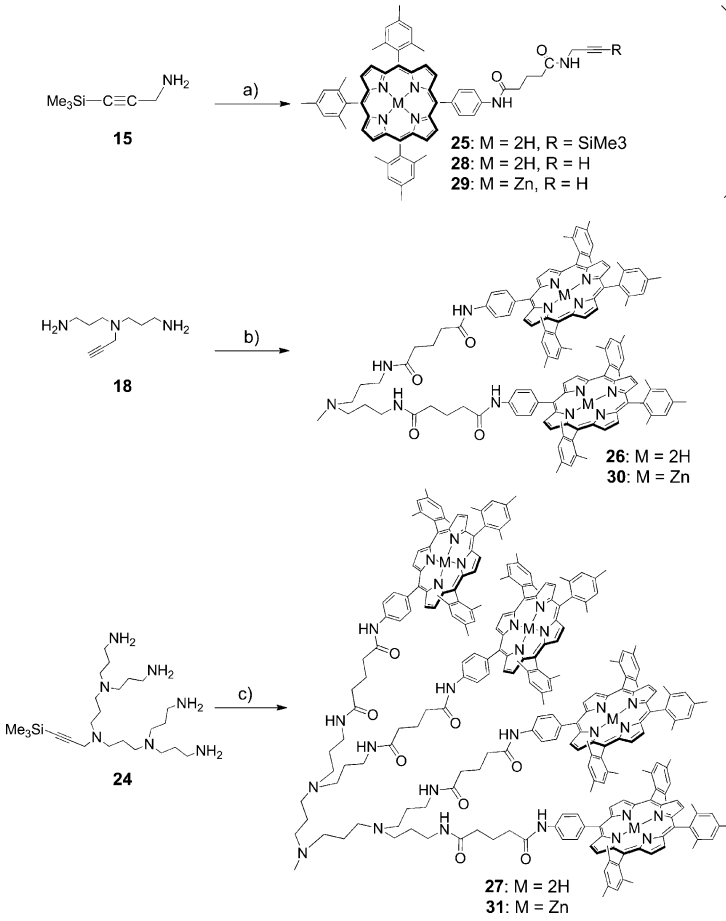

Scheme 7. Coupling reaction of active ester **14** (see Scheme 5) with the polypropylenimine dendrons. Reagents and conditions: a) **14**, CH_2Cl_2, RT, 18 h, then TBAF, THF, RT, 18 h, then $Zn(OAc)_2{\cdot}2H_2O$, $CHCl_3$/MeOH, reflux, 18 h; b) **14**, DIPEA, CH_2Cl_2, RT, 18 h, then $Zn(OAc)_2{\cdot}2H_2O$, $CHCl_3$/MeOH, reflux, 18 h; c) **14**, DIPEA, CH_2Cl_2, RT, 18 h, then $Zn(OAc)_2{\cdot}2H_2O$, $CHCl_3$/MeOH, reflux, 18 h.

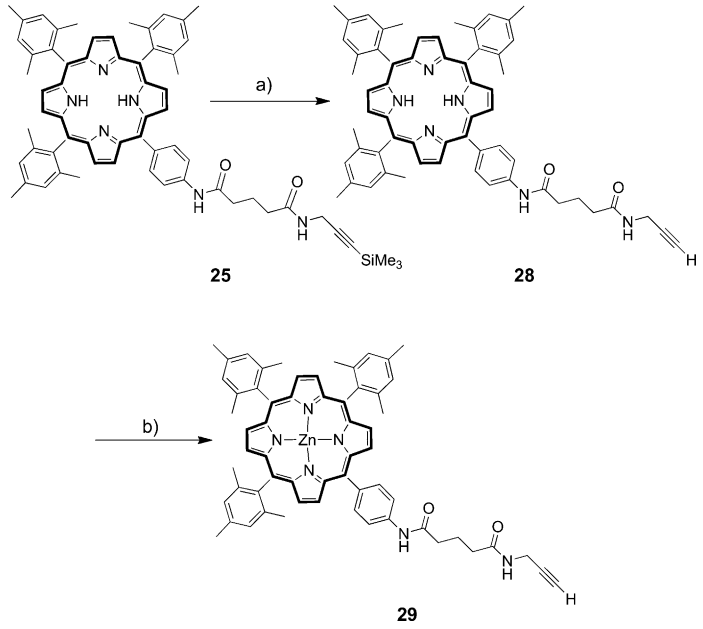

Scheme 8. Cleavage of the trimethylsilyl group and metalation of the **G1** dendron. Reagents and conditions: a) TBAF, CH_2Cl_2/THF (1:2), RT, 18 h; b) $Zn(OAc)_2{\cdot}H_2O$, $CHCl_3$/MeOH (10:1), RT, 18 h.

tional copper atoms, which were located in the porphyrin macrocycles of the cofacial bisporphyrin. The presence of the copper(II) porphyrin chromophore was confirmed by the UV/Vis spectra, which showed a strong blueshift of the Q bands. Details concerning the photophysical data are provided below. This known and anticipated reactivity is explained by the strong affinity of the porphyrin macrocycle for copper ions. Note that similar copper insertion has already been observed by Okada et al. in the case of a click-chemistry coupling between a free-base porphyrin with eight alkyne-terminals and β-lactosyl azides.[18] Marois et al. have shown that the use of Cu^{I} instead of the widely used Cu^{II} could avoid this metal insertion in the porphyrin core.[19] Nevertheless, Cu^{I}-catalyzed azide–alkyne 1,3-dipolar cycloadditions under classical conditions ($CuSO_4{\cdot}5H_2O$, sodium ascorbate) with free-base porphyrin have also been reported without any insertion of copper atom in the porphyrin.[20] This was not desirable at this stage of the research because of the rich photophysical properties offered by the copper(II) porphyrin chromophore, as described below.

A copper-catalyzed 1,3-dipolar cycloaddition was also induced between bisporphyrin diazide **9** and poly(propylene imine) alkyne dendrons **30** and **31**. The crude products were purified by preparative SEC chromatography to give dendrimers **34** and **35** in 48 and 72% yield, respectively (Scheme 9).

EPR studies: The EPR spectra of **33**–**35** (Figures S40–S42 in the Supporting Information) were also examined to determine whether the Cu···Cu separations remained unaltered upon anchoring the large dendrons. These can be estimated from the ratio of the intensity of the half-field transitions to

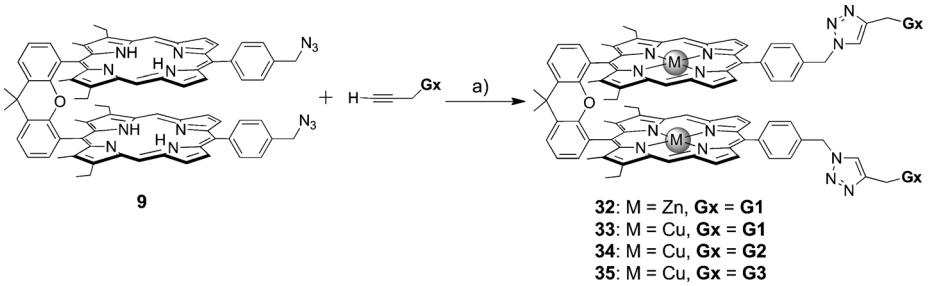

Scheme 9. Synthesis of dendrimers **32**–**35** by click chemistry. Reagents and conditions: a) **27** (**G1**), **28** (**G2**), or **29** (**G3**), CuI, DIPEA, CH_2Cl_2, RT, 18 h.

the intensity of the allowed transitions.[21] The $Cu^{II}\cdots Cu^{II}$ interactions at half-field transition were indeed noted in the EPR spectrum, but the signals were poorly resolved. The ratio of the intensity of the half-field transitions to the intensity of the allowed transitions are estimated to be 2.4×10^{-3} for **33**, 3.5×10^{-3} for **34**, and 1.5×10^{-3} for **35**, giving approximate interspin Cu···Cu distances of 4.5, 4.9, and 4.2 Å, respectively. These data are consistent with crystallographic data for copper xanthene-bridged cofacial bisporphyrins, $[Cu_2(DPX)]$ (3.910 Å),[6a,22] but the EPR analyses systematically provide higher values for metal–metal and interplanar separations, presumably owing to the absence of crystal-packing effects and π–π stacking in frozen solution.[23] However, in our case the lower resolution of the spectra and the resulting approximation does not allow reliable evaluation of the change in Cu···Cu separation as a function of the dendrimer size.

Spectroscopy and photophysics: Prior to describing the photophysical properties of the reported dendrimers, a description of the spectroscopic and photophysical properties of the copper(II) porphyrin chromophore is relevant. It has long been known that copper(II) porphyrin does not exhibit fluorescence, but rather a weak phosphorescence at room temperature is detected that becomes more intense as the temperature is lowered (see the Reference section). The two classic, most investigated examples are the copper(II) tetraphenylporphyrin ([Cu(TPP)]) and copper(II) etioporphyrin ([Cu(Etio)]).

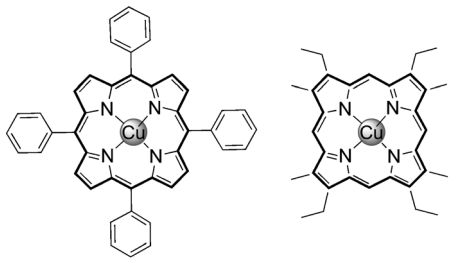

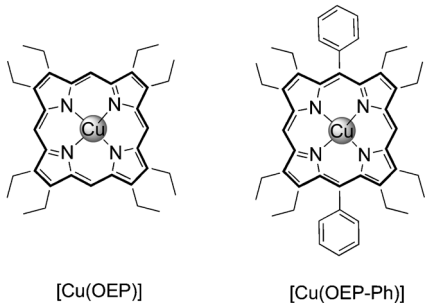

In the absence of fluorescence at room temperature, the kinetics of [Cu(TPP)] and [Cu(Etio)] were investigated by Holten et al. in the early days;[24] they established that the relaxation of the $^2S_1$ singlet state to the $^2T_1$ and $^4T_1$ trimultiplet states was operating on a ps timescale. This is due to a very efficient intersystem crossing process (triplet formation quantum yield, Φ_T, of 0.88 ± 0.02 in toluene).[25] The phosphorescence spectrum of [Cu(TPP)] at 77 K in methylcyclohexane shows an unstructured band at $\lambda=750$ nm.[26] This value was corroborated for a series of *meso*-substituted copper(II) porphyrins (R = aromatic, alkyl, or H) that exhibited phosphorescence lifetimes ranging from 15 to 300 ns (in CH_2Cl_2 at room temperature).[27] The position of the triplet state was also confirmed from the measurements of the absorption spectra focusing in the 700 nm region to observe the $^2S_0\rightarrow{}^2T_1$ transitions and the positions of these absorption features (295 K) and of the phosphorescence 0–0 peaks (77 K) for [Cu(TPP)] and copper(II) octaethylporphyrin ([Cu(OEP)]).[28] In toluene, these peaks were reported at $\lambda=688$ and 684 nm and at $\lambda=727$ and 683 nm, respectively.[28] In relation to this work, the position of these bands are $\lambda=686$ and 690 nm, respectively, for the mixed-substituent copper(II) *meso*,*meso*-diphenyl-octaethylporphyrin ([Cu(OEP-Ph)]). Because of the efficient triplet formation, investigations of this excited state revealed the presence of many triplet state phenomena, such as the presence of a lower-energy charge-transfer state (ring→metal) operating on the ps timescale,[29] the formation of an exciplex with water (among other donors)[30] also being formed on the ps timescale ((15 ± 5) ps),[31] the formation of singlet oxygen (see, for example, ref. [32]), the T_1–T_1 energy transfers to free bases,[33] and enhancement of intersystem crossing by through-bond exchange interactions.[34]

In the context of this work, zinc(II) tetraphenylporphyrin ([Zn(TPP)]) exhibits phosphorescence at $\lambda=778$ nm with a lifetime of 26 ms and a quantum yield of 0.012 at 77 K.[35] The relative positions of the phosphorescence at $\lambda=690$ nm for [Cu(OEP-Ph)] and $\lambda=778$ nm for [Zn(TPP)] (both structures are closely related to those used herein) predict that the copper- and zinc-containing units in the dendrimers should play roles as T_1–T_1 energy donors and acceptors, respectively. Furthermore, the possibility of enhancing the intersystem crossing of the zinc(II) porphyrin antenna in the dendrimers by through-bond exchange interactions with the copper-containing porphyrin is ruled out because these interactions are efficient between two and five conjugated bonds. Finally, the presence of electron transfer from a zinc(II) porphyrin to the Cu^{II} porphyrin chromophore assembled by a zinc–pyridine coordination bond or by ion-pair autoassembling was also invoked on the basis of thermodynamic arguments and ESR evidence.[36] In summary, the presence of copper(II) porphyrin leads to the possibility of both energy and electron transfer and enhancement of the intersystem-crossing rate constants of the neighboring chromophores.

Absorption: The UV/Vis data for the studied porphyrins are presented in Table 2, in which the intense Soret band (S_0–S_2 transition) and Q bands (S_0–S_1 transition) are characterized. Figure 2 shows a comparison between the UV/Vis spectra of the bisporphyrin (**33**) with that of the **G1** dendron zinc por-

Table 2. UV/Vis absorption data.

	λ_{max} [nm] ($\varepsilon \times 10^{-5}$ [$mol^{-1} L cm^{-1}$])			
	298 K		77 K	
	Soret band	Q bands	Soret band	Q bands
8	400 (1.27)	548 (0.06)	404 (2.20)	548 (0.13)
		586 (0.02)		588 (0.03)
29	424 (1.01)	556 (0.03)	428 (1.96)	558 (0.09)
		596 (0.01)		598 (0.04)
32	402 (0.10)	556 (0.01)	404	556 (0.17)
	426 (0.40)	594 (–)	428	594 (0.07)
30	404 (0.12)	558 (0.05)	406 (0.10)	514 (–)
	424 (1.58)	596 (–)	428 (1)	558 (0.06)
				596 (0.02)
34	394 (0.12)	558 (0.02)	396 (0.25)	556 (0.04)
	426 (0.42)	598 (0.01)	408 (0.12)	596 (0.02)
			428 (1)	
31	406 (0.08)	558 (0.04)	408 (0.22)	558 (0.13)
	426 (0.65)	596 (0.02)	428 (2.09)	596 (0.06)
35	398 (0.10)	558 (0.03)	396 (0.17)	556 (0.06)
	426 (0.72)	596 (–)	406 (0.16)	594 (0.03)
			428 (1)	
10	392 (1.15)	532 (0.04)	–	–
		568 (0.02)		
9	390 (1.30)	510 (0.06)	394 (1)	512 (0.06)
		546 (0.03)		548 (0.04)
		584 (0.03)		582 (0.03)
		634 (0.01)		632 (0.02)
25	418 (0.76)	514 (0.05)	402 (0.14),	514 (0.04)
		548 (0.03)	420 (1)	546 (0.02)
		592 (0.03)		588 (0.01)
		648 (0.02)		646 (0.02)
27	418 (1.21)	514 (0.05)	–	–
		548 (0.02)		
		594 (0.01)		
		656 (0.01)		
33	394 (0.49)	556 (0.05)	396 (0.64)	556 (0.02)
	426 (1)	592 (0.01)	428 (1)	594 (0.01)

phyrin (**29**), zinc bisporphyrin (**8**), and copper bisporphyrin (**10**). Figure 2, inset, shows the Q bands for these porphyrins. The absorption of bisporphyrin **33** shows features of both the **G1** dendron zinc porphyrin (**29**) and the copper bisporphyrin (**10**), which indicates a weak interaction between the two porphyrins. Furthermore, the absorption spectra of the different dendrimers clearly show no change on moving from one generation to the next, which reinforces the weak interaction between the porphyrin units.[1m]

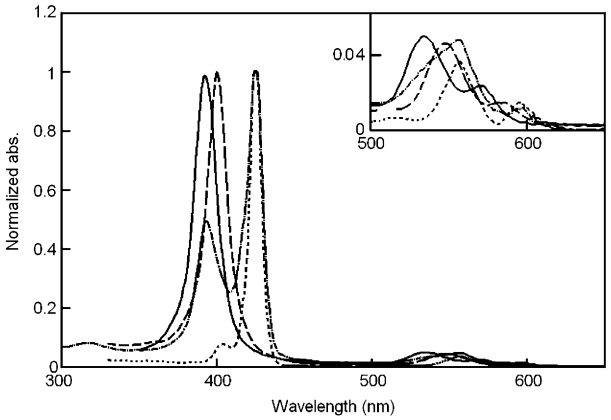

Figure 2. UV/Vis spectra of dendrimer **33** (–•–•), bis(copper(II) porphyrin) **10** (——), bis(zinc(II) porphyrin) **8** (– – –), and dendron **29** (-----) in 2MeTHF at 298 K. Inset: Enlarged view of the spectra between $\lambda = 500$ and 600 nm.

Fluorescence spectra: Typical examples of emissions from **G1** dendron **29** and dendrimers **32** and **33** in 2MeTHF at 77 and 298 K is given in Figure 3. The emission spectra recorded after excitation in the Q region exhibit $\pi\pi^*$ fluorescence typical of the zinc(II) porphyrin chromophore over the range of $\lambda = 600$ to 720 nm. The excitation spectra superimpose on the absorption ones, which confirms the identity of the fluorescence. No fluorescence was observed for bis(copper(II) porphyrin) **10**, which is normal for this porphyrin due to the rapid intersystem crossing, as mentioned above.[34] The fluorescence spectroscopic data for the investigated porphyrins are summarized in Table 3. Quantum yield measurements for the dendrimers and their precursors were carried out at 298 K in 2MeTHF and the obtained values are listed in Table 3.

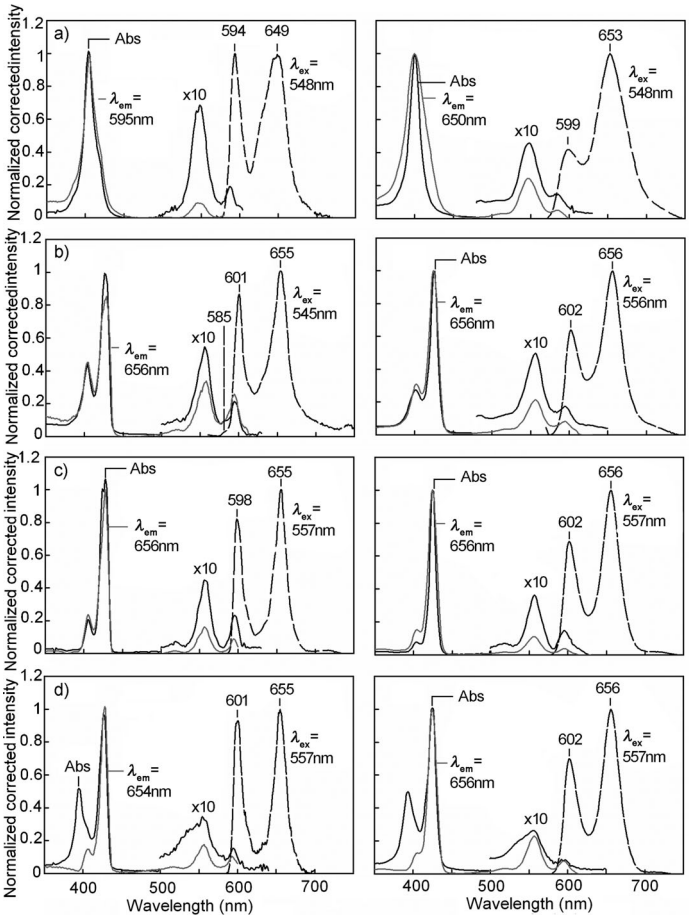

Figure 3. Emission (——), excitation (– – –), and absorption (——) spectra for a) zinc bisporphyrin **8**, b) bisporphyrin **32**, c) zinc **G1** dendron **29**, and d) bisporphyrin **33** in 2MeTHF at 77 (left) and 298 K (right).

Table 3. Luminescence data for the investigated porphyrins.

	Φ_F (±10%)[a]	λ_{max} [nm]	
		298 K	77 K
8	0.0072	599	594
		653	649
9	0.039	642	635
		706	703
10[b]	–	–	–
25	0.098	653	646
		722	717
29	0.041	602	598
		656	655
30	0.029	602	601
		656	657
		716 w	
31	0.030	602	602
		657	658
32	0.011		585
		602	601
		656	655
33	0.0096	602	601
		656	655
34	0.016	602	602
		657	657
35	0.017	602	602
		657	656

[a] Quantum yields measured in 2MeTHF at 298 K, with [Zn(TPP)] (TPP = tetraphenylporphyrin; $\Phi = 0.033$) as the reference.[37] The uncertainties for the quantum yields are ±10% based on multiple measurements. [b] Not luminescent.

Examination of the fluorescence quantum yields shows a decrease on moving from the precursors (**29**–**31**) to the dendrimers (**32**–**35**), which indicates the presence of an intramolecular excited-state interaction. Moreover, the quantum yield data for the porphyrin dendrimers increase in the order **G1** < **G2** < **G3**, which indicates a decrease in the interaction in the same order.

Transient absorption: The transient absorption signatures for the dendrimers and their synthons were recorded in 2MeTHF at 298 K and in the absence of oxygen. Figure 4 presents typical examples; the transient absorption spectra for the other compounds and dendrimers are provided in the Supporting Information. The transient spectra for **8** and **29** are very similar to each other and similar to other previously reported zinc(II) porphyrin systems, but we found that the relative absorbance varies despite very similar concentrations.[38] The spectra are characterized by a strong feature centered at $\lambda \approx 500$ nm (a peak at $\lambda \approx 490$ and a broad shoulder extending to $\lambda = 600$ nm), and are readily assigned to T_1–T_n absorption bands. The transient spectra of **32** and **33** are also very similar to those for **8** and **29** (and **30**, **31**, **34**, and **35**; see the Supporting Information), and the same T_1–T_n absorption band assignment can be readily made for them. No evidence of charge separation was observed.

Singlet excited state deactivation dynamics: Prior to performing emission lifetime measurements, singlet–singlet annihilation was considered because of the possible interactions between the zinc(II) tetra-*meso*-arylporphyrins. By using filters of neutral density, the fluorescence lifetimes (τ_F) of this chromophore were measured for several laser intensities, and were found to be independent of the filter. Fluorescence lifetimes for the porphyrin dimers and dendrons are presented in Table 4. The size of the fluorescence lifetimes and quantum yields for **8** and **9** are consistent with those reported for related derivatives H_4(DPX) and [Zn_2-

Table 4. Fluorescence lifetimes (τ_F) in 2MeTHF at 298 K and 77 K and in DMF at 298 K.

		2MeTHF				DMF	
		298 K		77 K		298 K	
	Φ_F[a]	χ^2	τ_F [ns]	χ^2	τ_F [ns]	χ^2	τ_F [ns]
8	0.007	0.98	2.27±0.25	0.86	2.38±0.06	0.85	1.79±0.07
9	0.039	1.23	13.58±0.15	1.21	17.39±0.03	–	–
25	0.098	0.91	14.77±0.24	0.93	15.86±0.19	–	–
29	0.041	1.24	2.33±0.01	0.75	2.84±0.06	0.91	2.06±0.02
30	0.029	0.96	2.31±0.02	0.96	2.75±0.03	1.09	1.99±0.01
31	0.030	1.02	2.27±0.02	1.09	2.47±0.04	0.77	1.97±0.02

[a] Quantum yield measured in 2MeTHF at 298 K. Uncertainties ±10%.

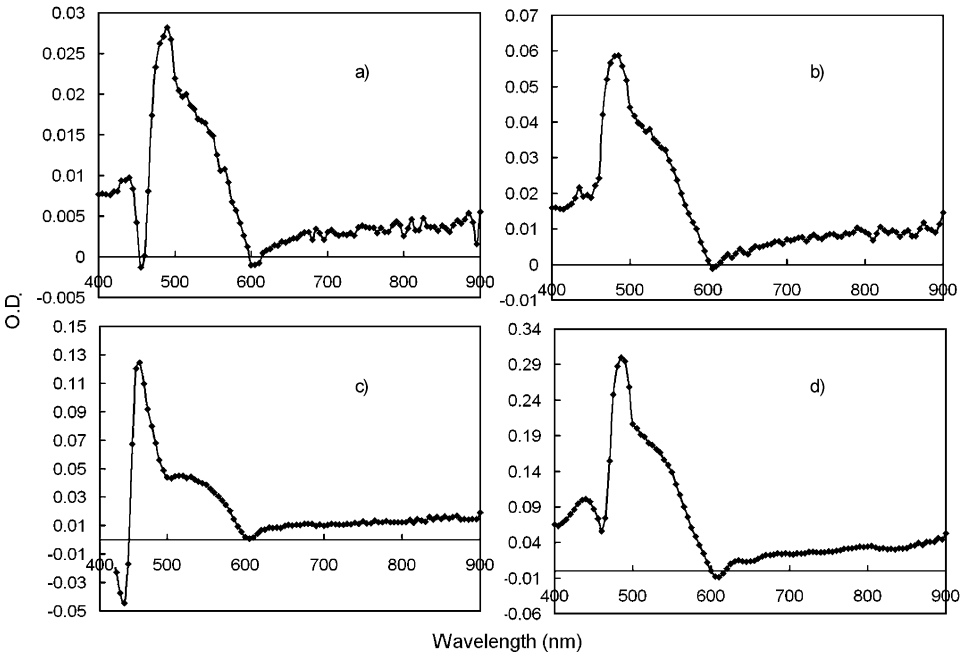

Figure 4. Transient absorption of a) dendrimer **33**, b) dendrimer **32**, c) zinc bisporphyrin **8**, and d) **G1** dendron **29** in 2MeTHF at 298 K. $\lambda_{ex} = 355$ nm right after laser-pump excitation. No delay time was employed for the recording of these spectra.

(DPX)].[4b] A comparison of the τ_F values for dendrons **29**, **30**, and **31** in 2MeTHF and DMF shows that they are very similar, but a weak decrease in τ_F is noted on moving from **29** to **30** to **31** (if neglecting the uncertainties), and also for Φ_F (from **29** to **30)**. This decrease is consistent with a slight increase in internal conversion associated with the increase in flexible groups near the chromophores. Note that the fluorescence lifetimes decrease by around 0.3 ns on going from 2MeTHF to DMF.

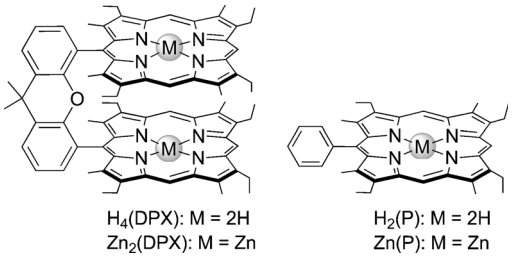

The decay traces of the fluorescence spectra exhibit a double exponential behavior for **32**, **33**, **34**, and **35**. This observation is, at first glance, counterintuitive, particularly for nonfluorescent copper-containing species **33**, **34**, and **35**. The analysis of the fluorescence decays for **32** indicates the presence of short- and long-lived components of around 0.4 and 2 ns, respectively, at both 298 and 77 K (with approximately the same amplitude at the selected monitoring wavelength; see details in Table 5). These values suggest one of the two chromophore fluorescence effects, either for bis(zinc(II) porphyrin) or zinc(II) tetra-*meso*-arylporphyrin, is quenched. In this case, no photoinduced electron transfer is observed, as demonstrated by the presence of T_1–T_n transient absorption described above and presented below in the absence of polarity and temperature effects for comparison, leaving only the singlet energy transfer as the only possible nonradiative process for intramolecular excited state deactivation. Similarly, an increase in internal conversion is also ruled out based on the weak effect observed above for dendrons **29**–**31**. Based on the positions of the absorption and fluorescence 0–0 peaks described above (see Tables 2 and 3), the bis(zinc(II) porphyrin) and zinc(II) tetra-*meso*-arylporphyrin act as the energy donor and acceptor, respectively. Using the fluorescence lifetime data for compounds **8** and **29** for comparison, the decrease in the τ_F value goes from ≈2.3 ns (for **8**) down to ≈0.4 ns in **32**. The longer component (≈1.5–2.5 ns) resembles those of compound **8** and dendron **29** (as well as **30** and **31**), and can be assigned to a weakly interacting chromophore. Because the τ_F data for compounds **8** and **29** are similar, it is difficult to deconvolute similar lifetimes in multicomponent decay traces. However, a proposed assignment is possible because the fluorescence quantum yields for **8** (0.7%) and **29** (4.1%) are different despite the similarity of the τ_F data. One intuitively assumes similarities in both the lifetimes and quantum yields by virtue of the assumed similarity of the fluorescence rate constant, k_F. However, in cofacial bisporphyrins (Scheme 10) the change in τ_F versus Φ_F is not necessarily linear, as recently demonstrated.[39] We assigned the long component of the fluorophore as arising mainly from the zinc(II) tetra-*meso*-arylporphyrin unit with a minor contribution from the bis(zinc(II) porphyrin) pair.

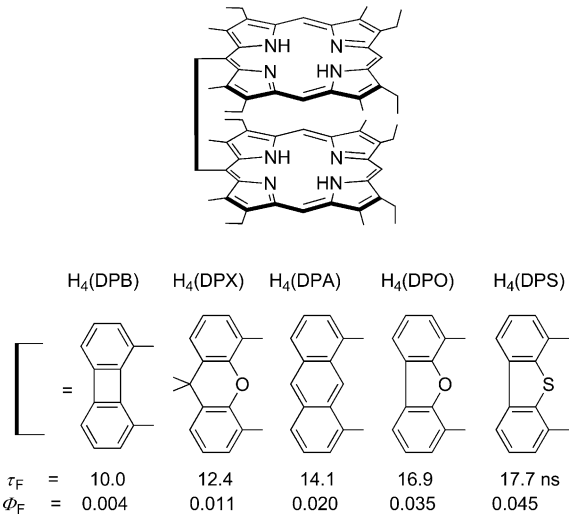

Scheme 10. τ_F and Φ_F values for different cofacial bisporphyrins.

Table 5. Fluorescence lifetimes, quantum yields, and rates of energy transfers of dyads.[a]

		2MeTHF				DMF	
	Φ_F[b]	τ_F [ns], 298 K (rel. intensity [%])[c]	τ_F [ns], 77 K (rel. intensity [%])[c]	S_1 k_{ET}[d] $[ns]^{-1}$ 298 K	77 K	τ_F [ns], 298 K (rel. intensity [%])[c]	S_1 k_{ET}[d] $[ns]^{-1}$ 298 K
32	0.011	0.36 ± 0.08 (50)	0.37 ± 0.08 (58)	2.3	2.3	0.33 ± 0.16 (40)	2.5
		1.90 ± 0.05 (50)	2.52 ± 0.08 (42)	–	–	1.47 ± 0.05 (60)	–
33	0.010	0.19 ± 0.01 (65)	0.21 ± 0.02 (78)	4.8	4.4	0.14 ± 0.09 (72)	6.7
		1.37 ± 0.03 (35)	2.24 ± 0.03 (22)	0.3	0.09	1.29 ± 0.02 (28)	0.3
34	0.016	0.38 ± 0.05 (60)	0.39 ± 0.05 (50)	2.2	2.2	0.31 ± 0.04 (90)	2.7
		1.61 ± 0.03 (40)	2.21 ± 0.05 (50)	0.2	0.09	1.86 ± 0.09 (10)	0.03
35	0.017	0.41 ± 0.03 (60)	0.48 ± 0.04 (70)	2.0	1.7	0.55 ± 0.13 (30)	1.3
		1.88 ± 0.03 (40)	2.34 ± 0.07 (30)	0.09	0.04	1.71 ± 0.04 (70)	0.08

[a] The fluorescence quenching rate constants are defined as k_{ET}, either as S_1–S_1 or S_1–T_1 (see text). [b] Quantum yields measured in 2MeTHF at 298 K (the uncertainties are ±10%). [c] The measurements were performed at the 0–0 peak of the donor in compound **32**, so a relative intensity of 50% is expected. For **33**, **34**, and **35**, the monitoring wavelength was the center of the zinc(II) tetra-*meso*-arylporphyrin fluorescence band to ensure better data. [d] The uncertainties are about ±0.3 ns^{-1} for the short component.

The comparison of the τ_F value of **32** with the τ_F values of dendrons **29–31** indicates that they are systematically shorter for practically all the experimental conditions, which means some excited state deactivation occurs. This increase in excited-state deactivation is likely to be due to internal conversion. Comparison with the data for **32** and **30** (two systems with two pendent zinc(II) tetra-*meso*-arylporphyrin units) indicates that this rate for deactivation would be of the order of $1–2\times10^8\ s^{-1}$ at 298 K and $0.3\times10^8\ s^{-1}$ at 77 K, which is consistent with an internal conversion process.

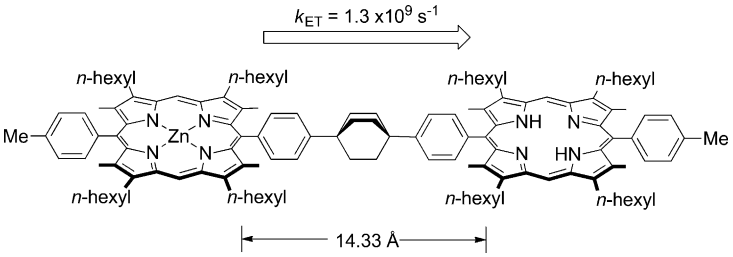

Scheme 12. Example of a rigidly held dyad.[47]

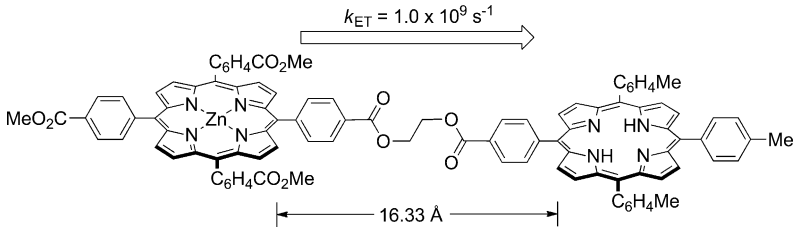

Scheme 13. Estimation of the donor–acceptor distance (PCModel) for a flexible dyad.[48]

By using the equation $k_{ET}=(1/\tau_F)-(1/\tau_F^o)$,[3] in which $\tau_F=1/(k_F+k_{ic}+k_{isc}+k_{ET})$ and $\tau_F^o=1/(k_F+k_{ic}+k_{isc})$ are the fluorescence lifetimes of the fluorophore in the presence (compound **32**; short component) and absence of energy transfer (compound **8**), respectively, the value of k_{ET} was estimated to be $\approx2.3\times10^9\ s^{-1}$ at both temperatures. The lack of temperature dependence of k_{ET} is consistent with the energy-transfer process. To verify whether or not electron transfer takes place in this case, measurements in DMF, a polar solvent that favors charge separation after the electron transfer, were also performed. The evaluated singlet k_{ET} value was $\approx2.5\times10^9\ s^{-1}$ and is essentially the same as that measured in 2MeTHF, a solvent of lower polarity. However, the size of the through-space singlet k_{ET} value (here $\approx2.4\times10^9\ s^{-1}$) seems to be too large (by ≈2–2.5 times; see below) for donor–acceptor distances of ≈20 Å (distance evaluated by computer modeling using PCModel; MMX; see Scheme 11). For comparison purposes, examples of known non-conjugated rigid and non-rigid dyads are presented in Schemes 12 and 13. The first example in Scheme 12[40] exhibits a rigidly held dyad in which both the donor (zinc(II)porphyrin) and acceptor (free base porphyrin) have β-alkyl groups that prevent the phenyl groups adopting a conformation favorable for conjugation. The *meso–meso* separation is around 14 Å and the rate for the singlet energy transfer was reported to be $1.3\times10^9\ s^{-1}$, which is slower than that measured for compound **32**. The second example in Scheme 13[41] has no β-alkyl groups and a flexible chain in the -C_6H_4-CO_2-CH_2CH_2-O_2C-C_6H_4- spacer, and thus is similar enough to **32** to allow appropriate comparison. The *meso–meso* separation is around 16 Å according to an energy-minimized conformation (PCModel). In this case, folding of this shorter and flexible spacer appears to be energetically unfavorable in the model. The rate for singlet energy transfer was reported to be $1.0\times10^9\ s^{-1}$, which is also slower than that measured for compound **32** but almost identical to the dyad illustrated in Scheme 12. The similarity in both the rate constants and the *meso–meso* separation for both compounds suggests that the *meso–meso* separation appears to be an adequate parameter for comparison purposes. Considering 20 Å as the donor–acceptor separation in compound **32**, the rate constant (again here $\approx2.4\times10^9\ s^{-1}$) does not follow the expected trend for the dyads shown in Schemes 12 and 13, for which a closer separation (14–16 Å) and slower rates constants ($\approx1\times10^9\ s^{-1}$) are noted.

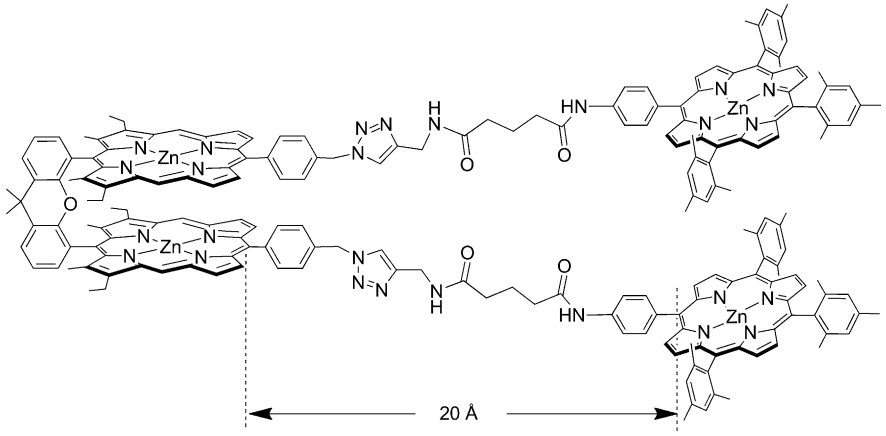

Scheme 11. Evaluation of the donor–acceptor distance in **32**.

Thus, a folding of the flexible chain in compound **32** must be considered, a folding that is probably driven by porphyrin stacking (Scheme 14). Indeed, computer modeling indicates a low-energy conformation, illustrated in Figure 5, which stresses the presence of short- and

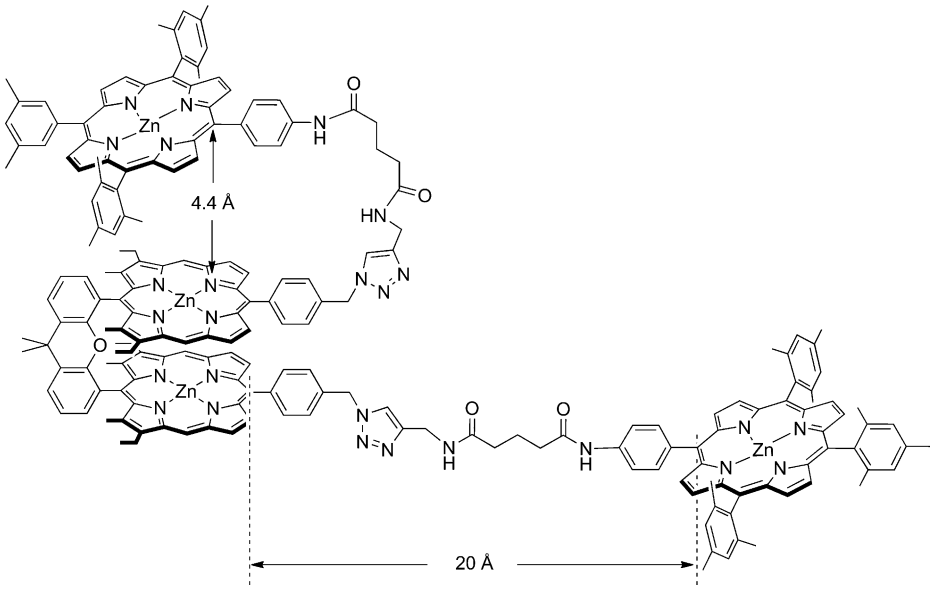

Scheme 14. Possible folding of a flexible chain in **32**; distances evaluated by using PCModel.

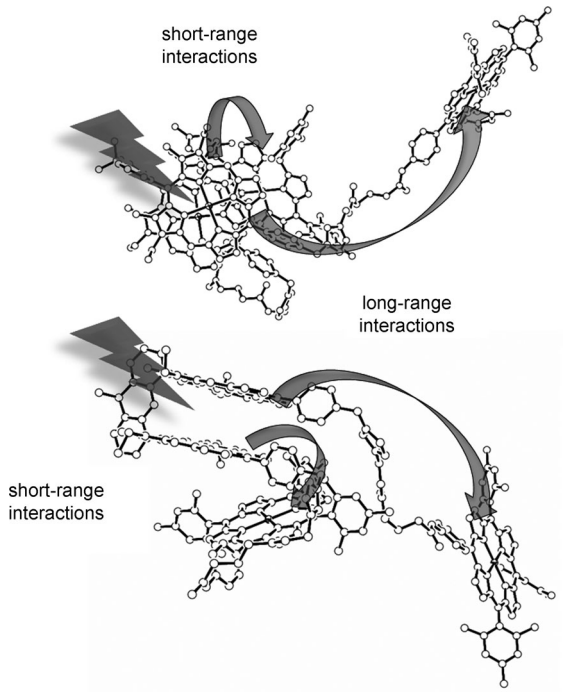

Figure 5. Computer model of compound **32** showing one possible conformation in which folding occurs, showing the presence of short- and long-range interactions. In this case, the calculated dihedral angle between the porphyrin and phenyl planes is ≈75°. The arrows indicate the direction of the transfer.

long-range interactions for singlet energy transfers in agreement with the experimental findings. An unambiguous evidence for this folding comes from the presence of triplet–triplet energy transfer discussed below.

The analysis of the excited-state dynamics of non-fluorescent copper-containing species **33**, **34**, and **35** is different from that of compound **32** because the possibility of both energy and electron transfers and enhancement of the intersystem-crossing rate constants of the neighboring chromophores must be considered, as previously mentioned. Again, the latter possibility has to be ruled out because this effect is a through-bond process that occurs over two to five conjugated bonds, which is not the case here. It was demonstrated above that a folded conformation best explains the biphasic decay behavior observed in compound **32**, thus this same phenomenon must be considered in the copper-containing dendrimers. We also considered the possibility of a through-space process, but such an event must be ruled out based on the following discussion. Indeed, a convincing argument comes from a comparison of the photophysical data of the free base in cofacial bis-etioporphyrins with the DPS spacer (dibenzothiophene; $d(meso–meso) = 6.33$ Å) with phenyl-etioporphyrin $H_2(P)$; Scheme 15).[4a] Indeed, no differences are observed between $H_2(P)$ and $H_4(DPS)$ and between $H_4(DPS)$ and $Pd(H_2(DPS))$, which indicates that neither the internal conversion nor intersystem-crossing non-radiative processes are affected by these structural modifications at this distance (and above), and the presence of a heavy atom (Pd) strongly favors intersystem crossing. The shortest Cu···C separation from Cu to the closest α-carbons of the zinc(II) tetra-*meso*-arylporphyrin in the folded conformation shown in Figure 5 is 6.70 Å based on computer modeling, which is longer than

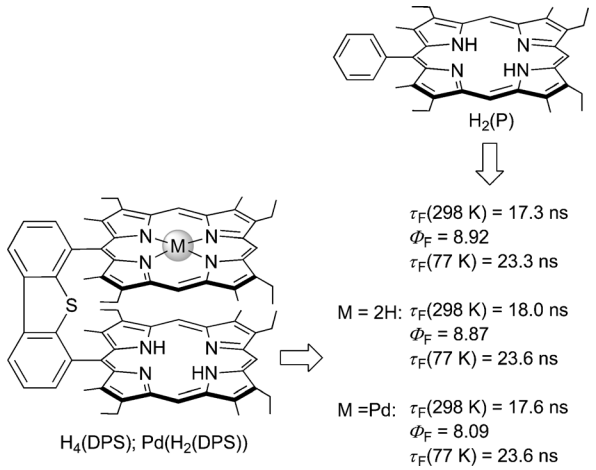

Scheme 15. Structures of $H_4(DPS)$, $PdH_2(DPS)$, and phenyl-etioporphyrin $H_2(P)$, and some of their photophysical data.

that for the DPS-containing system (6.33 Å) shown in Scheme 14. Such a separation is primarily driven by the size of the mesityl substituents, which prevent closer approach to the copper(II) center.

Because the quenching rate constant is temperature independent, somewhat weakly solvent dependent (there is even a decrease in rate constant in the more polar solvent for **35**), and again there is no evidence for signals associated to a charge-separated state, electron transfer is also excluded as an explanation of the fluorescence quenching. The last explanation is singlet–triplet energy transfer from the zinc(II) tetra-*meso*-arylporphyrin to the bis(copper(II) porphyrin), as illustrated in Figure 6. Singlet–triplet energy transfers

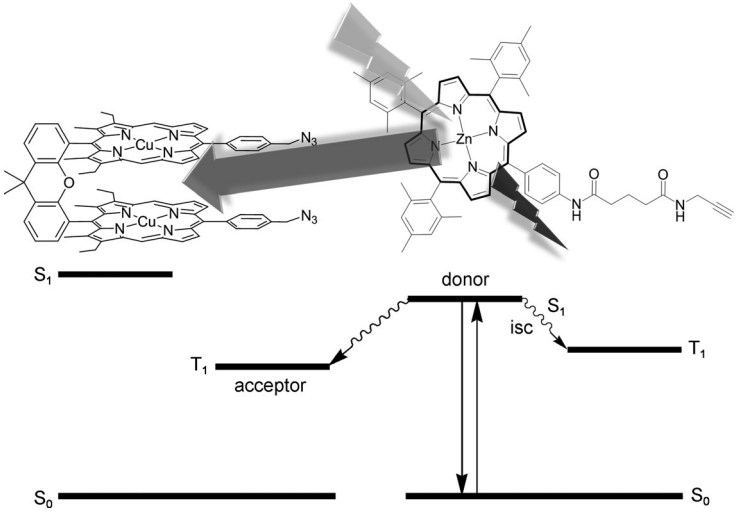

Figure 6. Diagram showing the singlet–triplet energy transfer process. The relative energy levels are based on the observed fluorescence and phosphorescence bands.

have often been observed in porphyrin-containing dyads.[42] The common feature of these reported dyads is that the porphyrin chromophore, generally zinc(II) porphyrin or the free base, is linked to a fragment prone to fast intersystem crossing, such as a heavy metal (e.g., ruthenium). Herein, this fragment is the paramagnetic Cu^{II}. The rate for singlet–triplet energy transfer decreases on going from **33** to **34** to **35** as the dendrimer gets larger. Based on modeling (see the Supporting Information), folding is possible but may be more difficult to achieve due to the longer chain length and the increase in the number of branches in the dendrons, which induces steric interactions between each other. Shorter-range interactions are possible in unfolded conformations, but these donor–acceptor separations may be longer than those described above for **33**, that is, longer that the M···C separation of 6.70 Å in **32** (M = Zn) and **33** (M = Cu).

Interestingly, the calculated quenching rate constants for the short component (i.e., closely placed donor–acceptor) is temperature independent for **33**–**35**, which is again consistent with an energy-transfer process. However, the longer component (i.e., for distant donors and acceptor) strongly suggests that the internal conversion dominates the deactivation. Consequently, S_1–T_1 energy transfer is slow but not zero because the calculated rates of deactivation (Table 5) are slightly larger than the internal conversion rate constants defined above for **32**; $1–2\times10^8\ s^{-1}$ at 298 K and $0.3\times10^8\ s^{-1}$. The k_{ET} values for the long components are reliably measurable.

Phosphorescence spectra and triplet-excited-state dynamics: The phosphorescence spectra and lifetimes (τ_F) for porphyrin dimer **10**, dendron **30**, and dendrimers **33**, **34**, and **35** are presented in Figure 7 and Table 6. The spectrum of dimer **10**

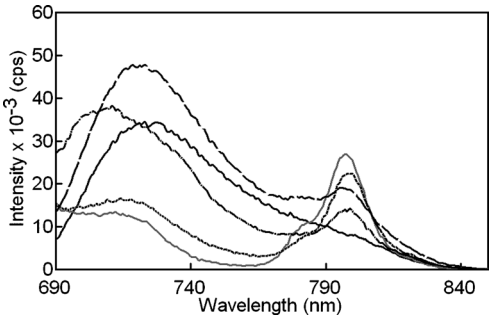

Figure 7. Phosphorescence emission of dimer **10** (——), dendron **30** (——), and dendrimers **33** (– – –), **34** (–•–•), and **35** (•••••) in 2MeTHF at 77 K, λ_{ex} = 570 nm.

Table 6. Phosphorescence data (peak positions and lifetimes).

	2MeTHF, 77 K	
	λ [nm]	τ_P [μs][a] (rel. intensity [%])
10	725, 790 sh	12.63 ± 1.34
33	725, 790 sh	1.73 ± 0.21 (75)
		13.3 ± 0.71 (25)
34	725, 790 sh	1.89 ± 0.02 (89)
		15.4 ± 0.03 (11)
35	800	too weak to be measured

[a] Measured at λ = 725 nm.

exhibits a maximum at λ = 725 nm and a shoulder at λ = 790 nm, which compares favorably with those discussed above for common copper(II) porphyrin species. The phosphorescence spectrum of dendron **30** exhibits a narrow band with a maximum at λ = 800 nm, which is also found in compound **35** by using time-resolved spectroscopy (Figure 8). The feature at λ = 715 nm belongs to the vibronic progression of the fluorescence arising from the zinc(II) tetra-*meso*-arylporphyrin unit. Thus three types of luminescence, phosphorescence of the donor and acceptor in the dyads, and fluorescence of zinc(II) tetra-*meso*-arylporphyrin unit are expected for compounds **33**, **34**, and **35**, which renders their spectra complex.

Time-resolved spectroscopy on the μs timescale permits a deconvolution of the low-and high-wavelength features. The much shorter lived fluorescence is obviously absent from the spectra on this timescale (Figure 8). For compound **10**,

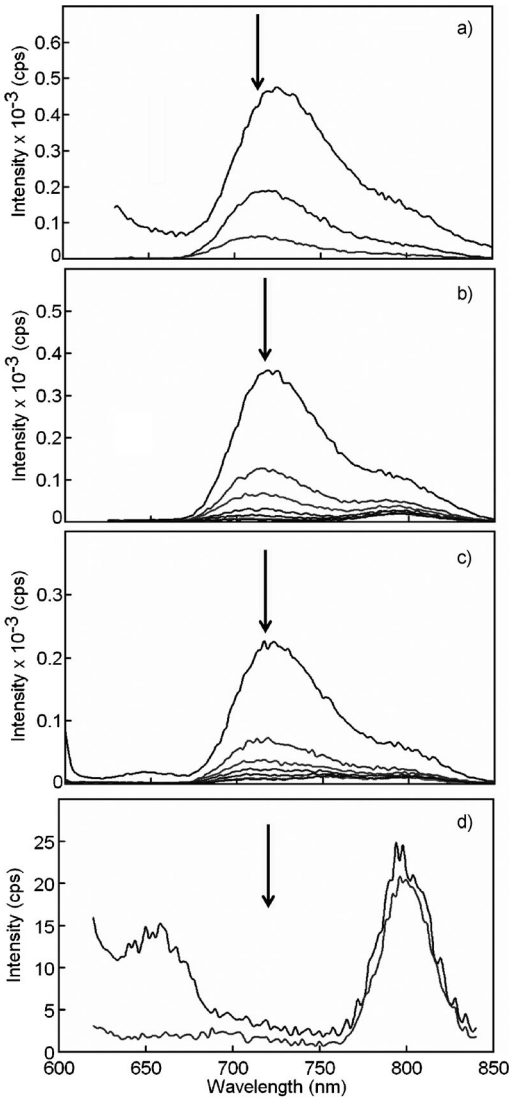

Figure 8. Time-resolved phosphorescence spectra of a) dendron **30** (delay time = 100, 120, 140 μs) and dendrimers b) **33** (delay time = 120, 140, 160, 200, 250, 300, 400 μs), c) **34** (delay time = 120, 140, 160, 180, 200, 230, 260 μs), and d) **35** (delay time = 120, 140 μs) in 2MeTHF at 77 K, λ_{ex} = 570 nm.

the time-resolved spectra show the expected maximum and shoulder that both decay with the same kinetics. However, for dendrimers **33** and **34** the phosphorescence band arising from the bis(copper(II) porphyrin) unit is also obvious but the low ($\lambda = 725$ nm) and high ($\lambda \approx 795$ nm) wavelength features do not decay at the same rate, which indicates the presence of two emissions. The shoulder decays at a slower rate, and at longer delay times only the $\lambda = 800$ nm feature is present. The lifetime for the phosphorescence of the zinc(II) porphyrin can be as long as 5760 μs.[4a] For compound **35**, only the long-lived $\lambda = 800$ nm band of the zinc(II) porphyrin is present (on the ms timescale), which indicates the presence of excited-triplet-state quenching of the bis(copper(II) porphyrin) fragment.

The triplet energy transfer rate constant ($k_{ET}(T_1)$) from the bis(copper(II) porphyrin donor to the zinc(II) porphyrin acceptor is estimated in a manner similar to that described above. Here, $k_{ET}(T_1) = (1/\tau_P) - (1/\tau_P^o)$,[3] in which $\tau_P = 1/(k_P + k_{ip} + k_{ET})$ and $\tau_P^o = 1/(k_P + k_{ip})$; k_P is the radiative rate constant of phosphorescence and k_{ip} is the non-radiative rate constant for internal conversion from the triplet state. Herein, the value of τ_P^o is ≈13 μs (Table 6; data for dimer **10**). The decays for **33** and **34** are also biphasic, which again indicates the short- and long-range interactions. For the long-lived component, the size of the phosphorescence lifetime (13–15 μs) indicates that no emission quenching occurs. On the other hand, the short component indicates evidence of quenching, with very similar rates of $\approx 5 \times 10^5\ s^{-1}$ for **33** and **34** after taking into account the uncertainties.[3] These values are consistent with the literature findings.[43] Indeed, relevant examples are shown in Scheme 16.[43]

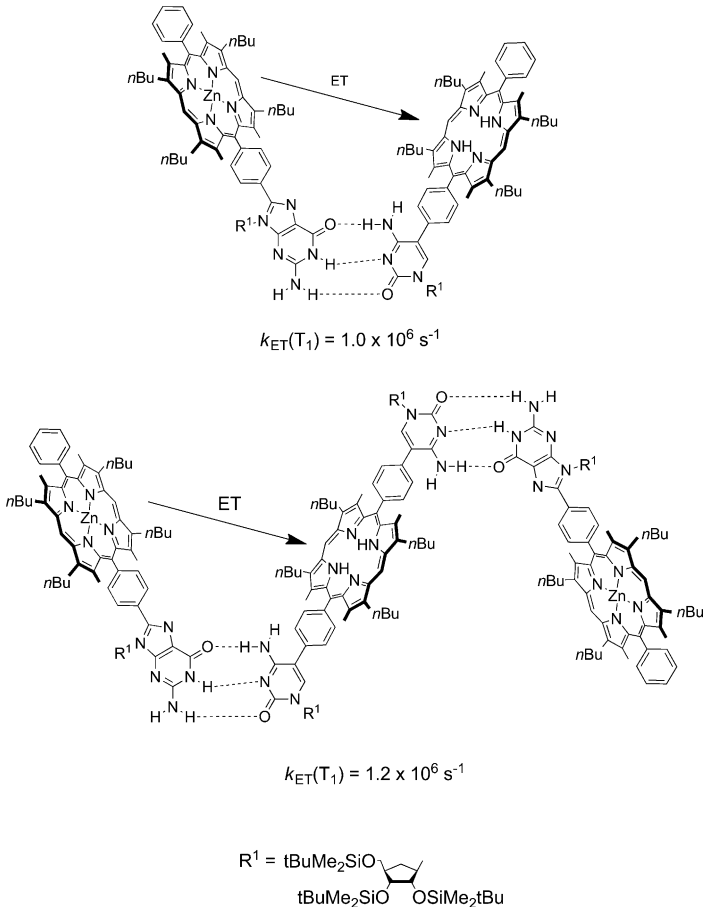

Scheme 16. Relevant examples of a dyad and a triad.[43]

One of the key issues of this work is the presence of chain folding to promote short-range interactions. It was recently demonstrated that the Dexter mechanism for singlet energy transfer was more effective at short distances.[4b] Similarly, given that the Dexter mechanism involves a double electron exchange between the donor and the acceptor, orbital over-

lap becomes important. It was recently demonstrated that above a certain limit, triplet energy transfer was no longer efficient after a certain distance.[4a] For example, triplet energy transfer from palladium(II) or platinum(II) porphyrins either occurs or doesn't according to the spacer used in cofacial systems (Scheme 17). This distance was estimated to be around 5 Å.

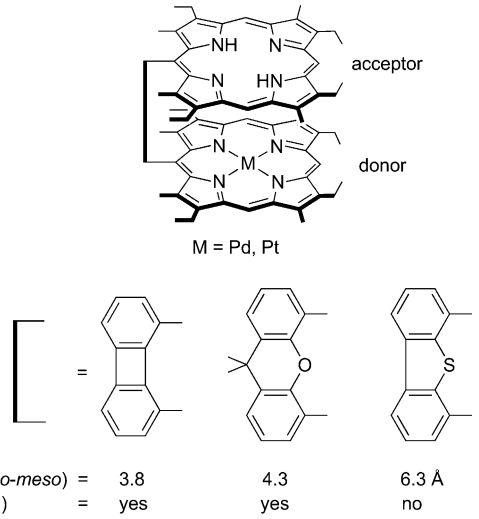

Scheme 17. Mono-palladium(II) and mono-platinum(II) bisporphyrins and triplet energy transfer rates.

For dendrimers **33**, **34**, and **35**, evidence of quenching from the decrease in phosphorescence lifetime or complete intensity quenching (in **35**) indicates triplet energy transfer because the T_1–T_n transient absorption signature is present at all times (see Figure S49 in the Supporting Information). This also means that, based on the Dexter mechanism (the concept of orbital overlap between the donor and acceptor), short distance interactions must exist and there one of the chains must be folded. Interestingly, the shortest atom–atom distances found for the computer model of **32** in Figure 5 are 4.2 (β-C···α-C), 4.3 (β-C···Zn), and 4.4 Å (β-C···N), which are within the approximate distance at which triplet energy transfer can be detected from phosphorescence lifetime measurements. The main conclusion from these measurements is that short-range interactions and chain folding exist in these dendrimers, as confirmed by computer modeling.

Conclusion

Dendrimers containing a central artificial special pair built upon a cofacial 9,9-dimethylxanthenebis(metal(II) porphyrin) (metal = zinc, copper) and three generations (**G1**, **G2**, **G3**) of zinc(II) tetra-*meso*-arylporphyrin-containing polyimide dendrons, connected by using click chemistry, were successfully synthesized and characterized. The interplanar distance between the two macrocycles in **8** is 3.46 Å in the solid state; this short distance closely mimics the interplanar distance found in the natural special pairs of cyanobacteria and purple photosynthetic bacteria.[3] Analysis of the photophysical properties, including transient absorption spectral behavior, indicates that the dendrons act as singlet and triplet energy acceptors or donors depending on the dendrimeric systems. The presence of the paramagnetic d^9 copper(II) in the dendrimers enriches the photophysical behavior by simultaneously promoting both singlet–triplet energy transfers from the zinc(II) tetra-*meso*-arylporphyrin to the non-fluorescent bis(copper(II)porphyrin) unit and slow triplet–triplet energy transfer from central bis(copper(II) porphyrin) fragment to the peripheral zinc(II) tetra-*meso*-arylporphyrin. If the central core is bis(zinc(II) porphyrin), evidence for chain folding is observed; this is unambiguously demonstrated by the presence of triplet energy transfer in the heterobimetallic systems, a process that only occurs at short distances. With respect to the antenna effect found around the natural special pairs of cyanobacteria and plants, the model investigated herein shows evidence of chain folding that brings the donor–acceptor assembly even closer together than similar systems found in Nature. In a way, the flexibility of the chain that adequately brings some porphyrin units close to the artificial special pair and others not is obviously desirable in the design of models, but the short interactions observed in the investigated dendrimers are in fact too short. We conclude that dendrimer design must aim for a system that prevents such a situation. This could be achieved through more rigid linkers or the presence of bulky groups around the chromophore at the periphery, or the presence of more hydrogen bonding within the chain in the case of inter-branch hydrogen bonds. Moreover, the timescale is slower by an order of magnitude in our models (200–400 ps) in comparison with 25–40 ps for natural photosystems, simply because chlorophylls are polar molecules[3] and, therefore, have a larger transition moment. Nonetheless, one can study such systems to better understand photosystems by changing one parameter at a time and observing the effect, something that cannot be done with natural systems.

Experimental Section

X-ray structure determination: Diffraction data were collected by using a Nonius Kappa Apex-II CCD diffractometer equipped with a low-temperature nitrogen jet stream system (Oxford Cryosystems). The X-ray source was graphite-monochromated $Mo_{K\alpha}$ radiation ($\lambda = 0.71073$ Å) from a sealed tube. The lattice parameters were obtained by least-squares fit to the optimized setting angles of the entire set of collected reflections. No significant temperature drift was observed during the data collections. Data were reduced by using DENZO software[44] without applying absorption corrections; the missing absorption corrections were partially compensated for by the data scaling procedure in the data reduction. The structure was solved by direct methods by using the SIR92 program.[45] Refinements were carried out by full-matrix least-squares on F^2 by using the SHELXL 97 program[46] for the complete set of reflections. Anisotropic thermal parameters were used for non-hydrogen atoms. All hydrogen atoms on carbon atom, were placed at calculated positions by using a

riding model with C–H = 0.98 Å (methyl), 0.99 Å (methylene), or 0.95 Å (aromatic) with $U_{iso}(H) = 1.5\,U_{eq}(CH_3)$, $U_{iso}(H) = 1.2\,U_{eq}(CH_2)$, or $U_{iso}(H) = 1.2\,U_{eq}(CH)$. One azide group exhibits disorder with a ratio of 0.52(1):0.48(1). The geometric parameters of disordered components in each group were constrained and restrained by using EADP[46–47] constraints and SAME[46–47] restraints. The displacement parameters of the other azide group were averaged by using the EADP[46–47] constraints because only the terminal nitrogen of the azide group had a slightly higher thermal motion.

X-ray crystal data for **8**: $C_{81}H_{68}N_{14}OZn_2$; $M_r = 1384.23$; triclinic; $P\bar{1}$; crystal size $0.20 \times 0.12 \times 0.02\ mm^3$; $a = 11.1916(2)$, $b = 13.6198(3)$, $c = 23.6362(6)$ Å; $V = 3264.90(12)$ Å^3; $\alpha = 93.8350(10)$, $\beta = 96.3930(10)$, $\gamma = 113.2660(10)°$; $Z = 2$; $\rho_{calcd} = 1.408\ Mg\,m^{-3}$; absorption coefficient $0.796\ mm^{-1}$; $F(000) = 1440$; θ range for data collection: 1.64–27.55°; 26198 reflns collected, 14841 independent reflns ($R_{int} = 0.0620$); completeness to $\theta = 27.55°$, 98.3 %; data/restraints/parameters: 14841/5/870; GOF on F^2: 1.127; final R indices [$I > 2\sigma(I)$]: $R_1 = 0.0763$, $wR_2 = 0.1381$; R indices (all data): $R_1 = 0.1158$, $wR_2 = 0.1581$.

CCDC-842542 (**8**) contains the supplementary crystallographic data for this paper. These data can be obtained free of charge from The Cambridge Crystallographic Data Centre via www.ccdc.cam.ac.uk/data_request/cif.

Instrumentation: Mass spectra were obtained by using a Bruker Ultraflex II instrument in MALDI-TOF reflectron mode with dithranol (1,8-dihydroxy-9[10*H*]-anthracene) as a matrix, or by using a Bruker MicroToFQ instrument in ESI mode. High-resolution mass spectroscopy (HRMS) was carried out by using a Bruker microTOF-Q ESI-TOF mass spectrometer. MALDI-TOF mass spectrometry of dendrimers **34** and **35** was carried out by using a Waters MALDI SYNAPT HDMS with dithranol as a matrix. EPR spectra were recorded in solution by using a Bruker ESP 300 spectrometer (Pôle de Chimie Moléculaire (Welience, UB-Filiale)) at the X-band (9.6 GHz) equipped with a double cavity and a liquid-nitrogen cooling accessory. EPR spectra were referenced to 2,2-diphenyl-1-picrylhydrazyl (DPPH; $g = 2.0036$).

UV/Vis spectra were recorded by using a Hewlett–Packard diode array (model 8452A) and the emission spectra were obtained by using a double-monochromator Fluorolog 2 instrument from Spex. The emission lifetimes were measured by using a TimeMaster Model TM-3/2003 apparatus from PTI. The source was a nitrogen laser with a high-resolution dye laser (fwhm ≈ 1600 ps) and fluorescence lifetimes were obtained from deconvolution or distribution lifetimes analysis. The flash photolysis spectra and the transient lifetimes were measured by using a Luzchem spectrometer with the $\lambda = 355$ nm line of a YAG laser from Continuum (Serulite) and the $\lambda = 530$ nm line from an OPO module pump by the same laser (fwhm = 13 ns).

Quantum yields: Measurements of quantum yields were performed in 2MeTHF at 298 K. Three different measurements (i.e., different solutions) were prepared for each photophysical datum (quantum yields and lifetimes). For 298 K measurements samples were prepared under an inert atmosphere (glovebox, $P_{O_2} < 25$ ppm). The sample and standard concentrations were adjusted to obtain an absorbance of 0.05 or less. The absorbance of the standard and the measured sample was adjusted to be as close as possible. Each absorbance value was measured five times for better accuracy in the measurements of the quantum yields. The reference used for quantum yield measurements was [Zn(TPP)] (TPP = tetraphenylporphyrin; $\Phi = 0.033$).[37]

Chemicals and reagents: All chemicals were purchased from Acros/Fisher Scientific, Aldrich or Alfa-Aesar (except Clarcel, purchased from SDS) and used as received without further purification. When needed, solvents were distilled and dried by standard methods. Silica gel 60 Å, SDS gel (70–120 μm), and Merck columns (35–70 μm) were used for column chromatography. Reactions were monitored by using thin-layer chromatography on commercial Merck 60 F254 silica gel plates (precoated sheets, 0.2 mm thick), UV/Vis spectra, and mass spectrometry. Size-exclusion chromatography (SEC) was carried out on a Bio-Rad Bio-Beads SX-1 column with CH_2Cl_2 as the eluent.

4,5-Bis[bis(4-ethyl-3-methyl-2-pyrryl)methyl]-9,9-dimethylxanthene (**3**),[6a] 4-(azidomethyl)benzaldehyde (**5**),[8] 3,4-dimethyl-1*H*-pyrrole-2-carbonic acid-*tert*-butyl ester,[48] *N*,*N*-bis(trifluoroacetyl)-1,7-diamino-4-azaheptane (**16**),[14] *N*-(*tert*-butoxycarbonyl)-1,7-diamino-4-azaheptane (**20**),[14] 5-mesityldipyrromethane,[12b] 5-(4-aminophenyl)-10,15,20-trimesitylporphyrin (**12**),[11] and 3-(trimethylsilyl)propargyl bromide[16] were synthesized as previously described.

5-[4-(Azidomethyl)phenyl]dipyrromethane (6): Pyrrole (45.0 mL, 64.4 mmol) and 4-(azidomethyl)benzaldehyde (1.07 g, 6.64 mmol) were added to a dry 250 mL round-bottomed flask and degassed with a stream of argon for 30 min. TFA (50.0 μL, 0.70 mmol) was added, and the solution was stirred under Ar at RT for 1 h. The reaction was quenched with NaOH (0.90 g) and stirred for 30 min. The mixture was vacuum filtered through Clarcel and excess pyrrole was removed under reduced pressure. The brown oil thus obtained was passed through a silica gel chromatography column (silica gel; CH_2Cl_2/*n*-heptane 1:1) to give the crude product as an yellow oil (1.22 g), which was used in the following steps without further purification. ^{1}H NMR (300 MHz, $CDCl_3$, 25 °C): $\delta = 7.83$ (br s, 2H; N*H*), 7.23 (d, J(H,H) = 8.3 Hz, 2H; phenyl-*H*), 7.18 (d, J(H,H) = 7.9 Hz, 2H; phenyl-*H*), 6.62 (m, 2H; α-pyrrole C*H*), 6.13 (m, 2H; β-pyrrole C*H*), 5.86 (m, 2H; β-pyrrole C*H*), 5.40 (s, 1H; C*H*), 4.28 ppm (s, 2H; CH_2); ^{13}C NMR (75.5 MHz, $CDCl_3$, 25 °C): $\delta = 142.4$, 134.1, 132.3, 128.9, 128.6, 117.5, 108.5, 107.4, 54.5, 43.7 ppm.

1,9-Diformyl-5-[4-(azidomethyl)phenyl]dipyrromethane (7): Under argon, in a 500 mL round bottom flask equipped with a reflux condenser and a septum, dry DMF (60 mL) was cooled with stirring for 15 min in an ice-water bath. $POCl_3$ (6.0 mL) was then added slowly. The ice bath was removed and the reaction mixture was stirred at RT for 30 min. The resulting red solution was cooled to 0 °C (ice bath) before addition of 5-[4-(azidomethyl)phenyl]dipyrromethane (6.04 g 21.8 mmol) in dry DMF (60 mL). After this addition, the reaction mixture was heated to 80 °C for 1 h. The resulting reddish mixture was allowed to cool to RT, at which point saturated aqueous NaOAc (180 mL) was added and the mixture was stirred for 20 min, then subsequently added to ice water. The solid that precipitated out as the result of this addition was isolated by filtration and washed with water until neutral pH was attained. After redissolution in ethyl acetate/*n*-heptane, the product was passed through a silica gel chromatography column (silica, ethyl acetate/*n*-heptane 3:7) to give the crude product as a yellow–orange powder (2.46 g) that was used without further purification for the following steps. ^{1}H NMR (300 MHz, DMSO, 25 °C): $\delta = 9.39$ (s, 2H; C*H*O), 7.83 (br s, 2H; N*H*), 7.32 (d, J(H,H) = 8.3 Hz, 2H; phenyl-*H*), 7.20 (d, J(H,H) = 8.1 Hz, 2H; phenyl-*H*), 6.93 (m, 2H; β-pyrrole C*H*), 6.02 (m, 2H; β-pyrrole C*H*), 5.63 (s, 1H; C*H*), 4.40 ppm (s, 2H; CH_2); ^{13}C NMR (75.5 MHz, DMSO, 25 °C): $\delta = 179.0$, 141.5, 141.0, 134.3, 132.6, 128.7, 128.5, 121.1, 110.2, 53.3, 42.8 ppm; MS (ESI): *m/z* calcd for $C_{18}H_{15}N_5O_2$: 334.1298; found: 334.1301 $[M+H]^+$.

4,5-Bis[zinc(II)(2,8-diethyl-3,7-dimethyl-15-[4-(azidomethyl)phenyl]-5-porphyrinyl)-9,9-dimethylxanthene (8): A suspension of 4,5-bis[(4,4′-diethyl-3,3′-dimethyl-2,2′-dipyrryl)methyl]-9,9′-dimethylxanthene (**3**; 328 mg, 0.49 mmol) and 1,9-diformyl-5-[4-(azidomethyl)phenyl]dipyrromethane (**7**; 270 mg, 0.81 mmol) in dry methanol (80 mL) was stirred under argon for 1 h. A solution of *p*-toluenesulfonic acid (1.00 g) in methanol (2 mL) was added dropwise to the stirred suspension over a 20 h period. The resulting dark-red solution was stirred in the dark for 72 h, then *p*-chloranil (300 mg) was added and the stirring was continued for a further 3 h. The reaction mixture was poured into saturated aqueous $NaHCO_3$ (80 mL) and extracted with CH_2Cl_2 (3 × 50 mL). The combined extract was washed with water (3 × 100 mL), dried over $MgSO_4$, and evaporated to dryness. The brown residue was redissolved in $CHCl_3$ (20 mL) and a saturated solution of zinc acetate in methanol (2 mL) was added. The resulting solution was stirred at RT for 18 h. After the solvent was removed under vacuum, the residue was taken up in dichloromethane and filtered through a silica gel pad. The silica was washed with dichloromethane until no more product was eluted. The solvent was removed in vacuo, and the crude material was purified by column chromatography (silica gel, CH_2Cl_2/*n*-heptane 7:3). Partial evaporation of the solvent removed mainly dichloromethane to yield pure **8** as a purple microcrystalline powder (25.2 mg, 0.04 mmol, 4.5 %). ^{1}H NMR (300 MHz, $CDCl_3$, 25 °C): $\delta = 9.04$ (m, 2H; *o*-phenyl-*H*), 8.62 (d, J(H,H) = 4.4 Hz, 4H; β-pyrrole

C*H*), 8.33 (d, *J*(H,H) = 4.4 Hz, 4H; β-pyrrole C*H*), 8.27 (s, 4H; *meso-H*), 7.97 (m, 2H; *m*-phenyl-*H*), 7.94 (m, 2H; Ar C*H*), 7.46 (m, 2H; *m*-phenyl-*H*), 7.38 (m, 2H; *o*-phenyl-*H*), 7.31 (t, *J*(H,H) = 7.6 Hz, 2H; Ar C*H*), 7.05 (m, 2H; Ar C*H*), 4.74 (s, 4H; 2×CH_2N$_3$), 3.35 (m, 8H; 4× ethyl CH_2), 2.35 (s, 12H; 4×methyl CH_3), 2.28 (s, 6H; 2×methyl CH_3), 1.38 ppm (t, *J*(H,H) = 7.6 Hz, 12H; 4×ethyl CH_3); UV/Vis (CH_2Cl_2): λ_{max} ($\varepsilon \times 10^{-3}$) = 396 (249), 541 (21.0), 578 nm (11.9 $mol^{-1}Lcm^{-1}$); MS (MALDI-TOF): *m/z* calcd for $C_{81}H_{69}N_{14}OZn_2$: 1385.43; found: 1385.31 $[M+H]^+$.

4,5-Bis[(2,8-diethyl-3,7-dimethyl-15-[4-(azidomethyl)phenyl]-5-porphyrin-yl)-9,9-dimethylxanthene (9): Compound **8** (80.7 mg, 58.2 μmol) was dissolved in dichloromethane (10 mL), then HCl (6 N, 10 mL) was added and the resulting mixture was stirred vigorously for 30 min. The organic layer was separated, washed with saturated aqueous $NaHCO_3$ (2×20 mL) and water (2×20 mL), and then dried over $MgSO_4$. The solvent was removed under reduced pressure to afford the title compound as a purple solid in quantitative yield (73.2 mg, 58.2 μmol). ^{1}H NMR (300 MHz, $CDCl_3$, 25 °C): δ = 8.93 (d, *J*(H,H) = 6.3 Hz, 2H; *o*-phenyl-*H*), 8.55 (d, *J*-(H,H) = 4.1 Hz, 4H; β-pyrrole C*H*), 8.32 (s, 4H; *meso-H*), 8.26 (d, *J*-(H,H) = 4.1 Hz, 4H; β-pyrrole C*H*), 7.96 (m, 4H; *m*-phenyl-*H* + Ar C*H*), 7.56 (d, *J*(H,H) = 7.4 Hz, 2H; *m*-phenyl-*H*), 7.47 (d, *J*(H,H) = 7.0 Hz, 2H; *o*-phenyl-*H*), 7.34 (t, *J*(H,H) = 6.9 Hz, 2H; Ar C*H*), 7.12 (d, *J*(H,H) = 6.5 Hz, 2H; Ar C*H*), 4.81 (s, 4H; 2×CH_2N$_3$), 3.46 (m, 8H; 4×ethyl CH_2), 2.36 (s, 12H; 4×methyl CH_3), 2.28 (s, 6H; 2×methyl CH_3), 1.39 ppm (t, *J*(H,H) = 7.2 Hz, 12H; 4×ethyl CH_3), NH (4H) not observed; UV/Vis (CH_2Cl_2): λ_{max} ($\varepsilon \times 10^{-3}$) = 391 (882), 511 (42.5), 546 (21.9), 580 (21.3), 634 nm (8.0 $mol^{-1}Lcm^{-1}$); MS (MALDI-TOF): *m/z* calcd for $C_{81}H_{73}N_{14}O$: 1257.61; found: 1257.62 $[M+H]^+$.

4,5-Bis[copper(II)(2,8-diethyl-3,7-dimethyl-15-[4-(azidomethyl)phenyl]-5-porphyrinyl)-9,9-dimethylxanthene (10): A solution of $Cu(OAc)_2{\cdot}2H_2O$ (29.0 mg) and sodium acetate (35.0 mg) in methanol (2 mL) was added to a solution of **8** (6.6 mg, 5.25 μmol) in chloroform (20 mL). The resulting solution was heated at reflux for 4 h, then the solvent was removed by rotary evaporation. The crude material was purified by column chromatography to give compound **10** (7.0 mg, 5.07 μmol, 98%). UV/Vis (CH_2Cl_2): λ_{max} ($\varepsilon \times 10^{-3}$) = 393 (447), 534 (14.6), 573 nm (5.4 $mol^{-1}Lcm^{-1}$); MS (MALDI-TOF): *m/z* calcd for $C_{81}H_{69}Cu_2N_{14}O$: 1381.44; found: 1381.39 $[M+H]^+$.

4-[4-(10,15,20-Trimesityl-porphyrin-5-yl)-phenylcarbamoyl]-butyric acid (13): Glutaric anhydride (302 mg, 2.51 mmol) was added to a solution of 5-(4-aminophenyl)-10,15,20-trimesitylporphyrin (**12**; 978 mg, 1.29 mmol) in dry CH_2Cl_2 (90 mL). The mixture was stirred at RT for 20 h, then concentrated under reduced pressure. The product was purified by column chromatography (silica gel, ethyl acetate) to afford the corresponding acid in quantitative yield (1.11 g, 1.28 mmol, >99%). ^{1}H NMR (300 MHz, $CDCl_3$, 25 °C): δ = 8.80 (d, *J*(H,H) = 4.8 Hz, 2H; β-pyrrole C*H*), 8.70 (d, *J*(H,H) = 4.8 Hz, 2H; β-pyrrole C*H*), 8.65 (s, 4H; β-pyrrole C*H*), 8.15 (d, *J*(H,H) = 8.1 Hz, 2H; phenyl-*H*), 7.86 (d, *J*(H,H) = 8.1 Hz, 2H; phenyl-*H*), 7.79 (s, 1H; N*H*CO), 7.29 (s, 6H; mesityl C*H*), 2.63–2.55 (m, 13H; 3×methyl CH_3 + CH_2CH_2CH_2), 2.18 (m, 2H; CH$_2$CH_2CH$_2$), 1.88 (s, 6H; 2×methyl CH_3), 1.86 (s, 12H; 4×methyl CH_3), −2.54 ppm (br s, 2H; N*H*); MS (MALDI-TOF): *m/z* calcd for $C_{58}H_{56}N_5O_3$: 870.44; found: 870.41 $[M+H]^+$.

4-[4-(10,15,20-Trimesityl-porphyrin-5-yl)-phenylcarbamoyl]-butyric acid 2,5-dioxopyrrolidin-1-yl-ester (14): 4-[4-(10,15,20-Trimesityl-porphyrin-5-yl)-phenylcarbamoyl]-butyric acid (**13**; 1.84 g, 2.11 mmol) was dissolved in anhydrous CH_2Cl_2 (56 mL) under argon, then cooled to 0 °C. Dicyclohexylcarbodiimide (480 mg, 2.33 mmol) and *N*-hydroxysuccinimide (240 mg, 2.09 mmol) were added. The reaction mixture was warmed to RT and stirred for 2 d. The solvent was evaporated and replaced with ethyl acetate to precipitate the dicyclohexylurea formed during the reaction. The organic layer was filtered and concentrated, then the crude product was purified by column chromatography (silica gel, $CHCl_3$) to give **14** as a violet solid (1.23 mg, 1.28 mmol, 60%). ^{1}H NMR (300 MHz, $CDCl_3$, 25 °C): δ = 8.82 (d, *J*(H,H) = 4.8 Hz, 2H; β-pyrrole C*H*), 8.69 (d, *J*(H,H) = 4.8 Hz, 2H; β-pyrrole C*H*), 8.64 (s, 4H; β-pyrrole C*H*), 8.41 (s, 1H; N*H*CO), 8.15 (d, *J*(H,H) = 8.4 Hz, 2H; phenyl-*H*), 7.94 (d, *J*(H,H) = 8.3 Hz, 2H; phenyl-*H*), 7.29 (s, 6H; mesityl C*H*), 2.94 (br s, 4H; COCH_2CH_2CO), 2.89 (m, 2H; CH_2CH$_2$CH$_2$), 2.67 (t, *J*(H,H) = 6.8 Hz, 2H; CH$_2$CH$_2$CH_2), 2.64 (s, 9H; 3×methyl CH_3), 2.36 (m, 2H; CH$_2$CH_2CH$_2$), 1.87 (s, 6H; 2×methyl CH_3), 1.86 (s, 12H; 4×methyl CH_3), −2.54 ppm (br s, 2H; N*H*); MS (MALDI-TOF): *m/z* calcd for $C_{62}H_{59}N_6O_5$: 967.45; found: 967.38 $[M+H]^+$.

3-Trimethylsilylprop-2-ynylamine (15): Hydrazine hydrate (0.85 mL, 17.5 mmol) was added to a suspension of *N*-[3-(trimethylsilyl)-2-propynyl]phthalimide (950 mg, 3.69 mmol) in dry ethanol (40 mL). The reaction mixture was heated at reflux for 2 h. After cooling, the precipitate of phthalic acid hydrazide was removed by filtration and washed with dichloromethane. The dichloromethane was removed under reduced pressure, but product **15** could not be separated from the ethanol by distillation. Therefore, it was left in solution and used directly in the following reaction steps. ^{1}H NMR (300 MHz, $CDCl_3$, 25 °C): δ = 4.82 (br s, 2H; N*H*), 3.36 (s, 2H; CH_2), 0.09 ppm (s, 9H; Si(CH_3)$_3$); ^{13}C NMR (75.5 MHz, $CDCl_3$, 25 °C): δ = 106.9, 86.9, 32.2, −0.09 ppm; MS (ESI): *m/z* calcd for $C_6H_{13}NSi$: 128.09; found:128.11 $[M+H]^+$.

***N*^{4}-(Prop-2-ynyl)-*N*^{1},*N*^{7}-bis(trifluoroacetyl)-1,7-diamino-4-azaheptane (17)**: A solution of propargyl bromide in toluene (80%, 3.8 mL, 35.3 mmol) was slowly added to a solution of *N*^{1},*N*^{7}-bis(trifluoroacetyl)-1,7-diamino-4-azaheptane (**16**; 8.53 g, 26.4 mmol) and triethylamine (5.50 mL, 39.6 mmol) in dry THF (100 mL). The mixture was stirred at RT for 3 d. The reaction mixture was poured into saturated aqueous $NaHCO_3$ (100 mL) and extracted with $CHCl_3$ (3×100 mL). The combined organic layers were washed with brine, dried over $MgSO_4$, and evaporated under reduced pressure to give **17** as a red oil (5.25 g, 14.5 mmol, 55%). ^{1}H NMR (300 MHz, $CDCl_3$, 25 °C): δ = 7.73 (s, 2H; N*H*), 3.44 (dt, *J*(H,H) = 6.2 Hz, *J*(H,H) = 6.1 Hz, 4H; NHCH_2CH$_2$), 3.38 (d, *J*(H,H) = 2.3 Hz, 2H; NCH_2CCH), 2.60 (t, *J*(H,H) = 6.4 Hz, 4H; CH$_2$CH_2N), 2.21 (t, *J*(H,H) = 2.3 Hz, 1H; CC*H*), 1.72 ppm (m, 4H; CH$_2$CH_2CH$_2$); ^{13}C NMR (75.5 MHz, $CDCl_3$, 25 °C): δ = 157.5 (q, *J*(C,F) = 37 Hz, *C*OCF$_3$), 116.1 (q, *J*(C,F) = 288 Hz, *C*F$_3$), 77.2 (CH$_2$*C*CH), 73.9 (*C*CH), 51.8 (CH$_2$*C*H$_2$N), 41.1 (N*C*H$_2$CCH), 38.9 (NH*C*H$_2$CH$_2$), 25.7 ppm (CH$_2$*C*H$_2$CH$_2$); HRMS (ESI): *m/z* calcd for $C_{13}H_{18}F_6N_3O_2$: 362.1298; found: 362.1290 $[M+H]^+$.

***N*-(Prop-2-ynyl)-1,7-diamino-4-azaheptane (18)**: *N*-(Prop-2-ynyl)-*N*,*N*-bis(trifluoroacetyl)-1,7-diamino-4-azaheptane (**17**; 696 mg, 1.61 mmol) was treated with a mixture of MeOH and NH_4OH (25%, 18 mL, 1:2) and heated at reflux for 20 h. The residue was dried under high vacuum to give product **18** as a colorless oil (272 mg, quantitative). ^{1}H NMR (300 MHz, MeOD, 25 °C): δ = 3.46 (d, *J*(H,H) = 2.4 Hz, 2H; NCH_2CCH), 3.35 (s, 4H; N*H*), 2.99 (t, *J*(H,H) = 7.5 Hz, 4H; CH$_2$CH_2N), 2.64 (t, *J*-(H,H) = 6.8 Hz, 4H; CH$_2$CH_2N), 2.63 (s, 1H; CC*H*), 1.82 ppm (tt, *J*-(H,H) = 6.8, 7.5 Hz, 4H; CH$_2$CH_2CH$_2$); HRMS (ESI): *m/z* calcd for $C_9H_{20}N_3$: 170.1652; found: 170.1649 $[M+H]^+$.

***N*-Tetra-alkylation of compound 20 by *N*-(3-bromopropyl)phthalimide (21)**: A suspension of *N*^{4}-(*tert*-butoxycarbonyl)-1,7-diamino-4-azaheptane (**20**; 1.52 g, 6.58 mmol) and K_2CO_3 (4.56, 33.0 mmol) in acetonitrile (275 mL) was heated at reflux for 2 h. *N*-(3-Bromopropyl)phthalimide (8.84 g, 33.0 mmol) was added and the reaction mixture was stirred for 2 d. After cooling to RT, the solid was filtered and the solvent was evaporated. The remaining oil was extracted with CH_2Cl_2/water and washed with water. The organic layer was dried over $MgSO_4$. The crude product was purified by column chromatography (silica gel, $CHCl_3 \rightarrow 5\%$ MeOH/95% $CHCl_3$) to give **21** (4.47 g, 4.52 mmol, 69%). ^{1}H NMR (300 MHz, $CDCl_3$, 25 °C): δ = 7.73–7.59 (m, 16H; Pht), 3.64 (t, *J*(H,H) = 7.2 Hz, 8H; CH_2NPht), 3.13 (m, 4H; NCH_2CH$_2$), 2.43 (t, *J*(H,H) = 6.6 Hz, 8H; NCH_2CH$_2$), 2.36 (t, *J*(H,H) = 7.0 Hz, 4H; CH$_2$CH_2N), 1.73 (m, 8H; CH$_2$CH_2 CH$_2$), 1.60 (m, 4H; CH$_2$CH_2CH$_2$), 1.36 ppm (s, 9H; *t*Bu-CH_3); ^{13}C NMR (75.5 MHz, $CDCl_3$, 25 °C): δ = 168.2, 155.4, 133.7, 132.1, 123.0, 78.9, 51.3, 51.2, 45.6, 36.3, 28.4, 26.1, 25.8 ppm; HRMS (ESI): *m/z* calcd for $C_{55}H_{62}N_7O_{10}$: 980.4553; found: 980.4586 $[M+H]^+$.

Compound 22: Compound **21** (2.25 g, 2.30 mmol) was dissolved in $CHCl_3$ (6.8 mL), then TFA (18.2 mL) was slowly added at 0 °C. After stirring for 5 h, the solvent and the TFA were removed under vacuum. The resulting residue was dissolved in water and adjusted to pH > 8 by addition of saturated aqueous $NaHCO_3$. The resulting solution was extracted with $CHCl_3$ (5×20 mL) and the combined organic layers were dried over $MgSO_4$, fil-

tered, and concentrated in vacuum to give **22** (949 mg, 1.08 mmol, 47%). ^{1}H NMR (300 MHz, $CDCl_3$, 25°C): δ = 7.69–7.64 (m, 8H; Pht), 7.61–7.56 (m, 8H; Pht), 3.64 (t, J(H,H) = 7.3 Hz, 8H; CH_2NPht), 3.25 (t, J(H,H) = 7.1 Hz, 4H; NCH_2CH$_2$), 2.55 (t, J(H,H) = 5.7 Hz, 4H; CH$_2$CH_2N), 2.47 (t, J(H,H) = 6.6 Hz, 8H; NCH_2CH$_2$), 2.03 (m, 4H; CH$_2$CH_2CH$_2$), 1.74 ppm (m, 8H; CH$_2$CH_2CH$_2$), NH not observed; ^{13}C NMR (75.5 MHz, $CDCl_3$, 25°C): δ = 168.2, 133.8, 131.9, 123.1, 57.7, 51.1, 47.5, 36.1, 25.9, 23.6 ppm; HRMS (ESI): *m/z* calcd for $C_{50}H_{54}N_7O_8$: 880.4028; found: 880.4042 $[M+H]^+$.

Compound 23: 3-(Trimethylsilyl)propargyl bromide (118 mg, 0.62 mmol) and K_2CO_3 (373 mg, 2.70 mmol) were added to a solution of compound **22** (544 mg, 0.62 mmol) in dry acetonitrile (50 mL). The resulting reaction mixture was heated at 40°C for 48 h, then filtered and the filtrate was concentrated. The crude product was purified by column chromatography (silica gel, $CHCl_3$→2% MeOH/98% $CHCl_3$) to give **23** (383 mg, 0.39 mmol, 63%). ^{1}H NMR (300 MHz, $CDCl_3$, 25°C): δ = 7.82–7.76 (m, 8H; Pht), 7.70–7.63 (m, 8H; Pht), 3.70 (t, J(H,H) = 7.4 Hz, 8H; CH_2NPht), 3.35 (s, 2H; CH_2CC), 2.50–2.40 (m, 16H; 2× CH$_2$CH_2N, 4× NCH_2CH$_2$, 2× NCH_2CH$_2$), 1.78 (m, 8H; CH$_2$CH_2CH$_2$), 1.53 (m, 4H; CH$_2$CH_2CH$_2$), 0.12 ppm (s, 9H; TMS-CH_3); ^{13}C NMR (75.5 MHz, $CDCl_3$, 25°C): δ = 168.4, 133.9, 132.3, 123.2, 101.3, 89.7, 51.9, 51.8, 51.5, 42.8, 36.6, 26.3, 24.8, 0.3 ppm; HRMS (ESI): *m/z* calcd for $C_{56}H_{64}N_7O_8Si$: 990.4580; found: 990.4626 $[M+H]^+$.

Compound 24: Hydrazine hydrate (0.29 mL, 5.97 mmol) was added to a suspension of *N*-[3-(trimethylsilyl)-2-propynyl]phthalimide (361 mg, 0.36 mmol) in dry ethanol (10 mL). The reaction mixture was heated at reflux for 3 h. After cooling, the precipitate of phthalic acid hydrazide was removed by filtration and washed with dichloromethane. The solvents were evaporated under reduced pressure to dryness to give **24** (169 mg, 0.36 mmol, 99%) as a yellow oil. ^{1}H NMR (300 MHz, CD_3OD, 25°C): δ = 3.44 (s, 2H; CH_2CC), 2.73 (t, J(H,H) = 7.0 Hz, 8H; CH_2NH$_2$), 2.55–2.45 (m, 16H; 2× CH$_2$CH_2N, 4× NCH_2CH$_2$, 2× NCH_2CH$_2$), 1.72–1.61 (m, 12H; 4× CH$_2$CH_2CH$_2$, 2× CH$_2$CH_2CH$_2$), 0.15 ppm (s, 9H; TMS-CH_3); ^{13}C NMR (75.5 MHz, CD_3OD, 25°C): δ = 101.8 (CCSiMe$_3$), 90.8 (CH$_2$$C$C), 52.9, 52.7 (4× NCH$_2CH_2$, 2× NCH$_2CH_2$, 2× NCH$_2CH_2$), 43.3 (N$CH_2$C), 40.7 (C$H_2NH_2$), 29.2 (4× CH$_2CH_2CH_2$), 25.2 (2× CH$_2CH_2CH_2$), 0.2 ppm (TMS-C$H_3$).

Protected G1 dendron (25): Porphyrinic activated ester **14** (331 mg, 0.34 mmol) was dissolved in dry dichloromethane (15 mL) under argon, then a solution of *N*-[3-(trimethylsilyl)-2-propinyl]amine (**15**; 0.76 mmol) in ethanol (400 µL) was added. The resulting reaction mixture was stirred at RT for 18 h. The solvent was removed under reduced pressure and the crude material was purified by column chromatography (silica gel, $CHCl_3$). The fractions were monitored by using TLC and the pure title compound was isolated as a purple solid (121 mg, 0.12 mmol, 36%). ^{1}H NMR (300 MHz, $CDCl_3$, 25°C): δ = 8.83 (d, J(H,H) = 4.7 Hz, 2H; β-pyrrole CH), 8.70 (d, J(H,H) = 4.7 Hz, 2H; β-pyrrole CH), 8.50 (s, 1H; CONHCH$_2$), 8.18 (d, J(H,H) = 8.0 Hz, 2H; phenyl-H), 7.97 (d, J(H,H) = 8.0 Hz, 2H; phenyl-H), 7.94 (s, 4H; β-pyrrole CH), 7.29 (s, 6H; mesityl CH), 6.00 (s, 1H; NHCOCH$_2$), 4.18 (d, J(H,H) = 4.8 Hz, 2H; NHCH_2), 2.68 (t, J(H,H) = 6.6 Hz, 2H; CH_2CH$_2$CH$_2$), 2.64 (s, 9H; 3× methyl CH_3), 2.52 (t, J(H,H) = 6.5 Hz, 2H; CH$_2$CH$_2$CH_2), 2.23 (m, 2H; CH$_2$CH_2CH$_2$), 1.88 (s, 6H; 2× methyl CH_3), 1.87 (s, 12H; 4× methyl CH_3), 0.21 (s, 9H; Si(CH_3)$_3$), −2.54 ppm (brs, 2H; NH); MS (MALDI-TOF): *m/z* calcd for $C_{64}H_{67}N_6O_2Si$: 979.51; found: 979.40 $[M+H]^+$.

Zinc G1 dendron (29): Compound **25** (30.2 mg, 29.0 µmol) was dissolved in CH_2Cl_2/THF (1:2 v:v, 6 mL) at RT and treated with an excess of TBAF (1 M) in THF (274 µL, 274 µmol). The resulting solution was stirred at RT for 18 h, then the solvent was evaporated and replaced with $CHCl_3$ (10 mL). A saturated solution of zinc acetate in methanol (1 mL) was added and the solution was heated at reflux for 1 h. After the solvent was removed, the residue was taken up in chloroform and purified by using column chromatography (silica gel, $CHCl_3$) to give the title compound as a purple solid (26.8 mg, 27.6 µmol, 95%). ^{1}H NMR (300 MHz, [D$_8$]THF, 25°C): δ = 9.58 (brs, 1H; NHCOCH$_2$), 8.80 (d, J(H,H) = 4.6 Hz, 2H; β-pyrrole CH), 8.62 (d, J(H,H) = 4.6 Hz, 2H; β-pyrrole CH), 8.61 (s, 4H; β-pyrrole CH), 8.05 (brs, 2H; phenyl-H), 8.04 (brs, 2H; phenyl-H), 7.59 (brs, 1H; NHCOCH$_2$), 7.28 (brs, 6H; mesityl CH), 4.02 (m, 2H; NHCH_2), 2.59 (brs, 9H; 3× methyl CH_3), 2.53 (t, 2H; J(H,H) = 7.0 Hz, CH_2CH$_2$CH$_2$), 2.35 (t, 2H; J(H,H) = 7.0 Hz, CH$_2$CH$_2$CH_2), 2.09 (m, 3H; CH$_2$CH_2CH$_2$, CCH), 1.85 ppm (brs, 18H; 6× methyl CH_3); UV/Vis (CH_2Cl_2): λ_{max} ($\varepsilon\times10^{-3}$) = 421 (672), 550 (25.6), 588 nm (3.1 mol^{-1} L cm^{-1}); MS (MALDI-TOF): *m/z* calcd for $C_{61}H_{56}N_6O_2Zn$: 968.38; found: 968.35 $[M]^{+\cdot}$.

G2 dendron (26): *N*$^-$(Prop-2-ynyl)-1,7-diamino-4-azaheptane (**18**; 75.5 mg, 0.45 mmol) and the porphyrinic activated ester (**14**; 862 mg, 0.89 mmol) were dissolved in dry CH_2Cl_2 (19 mL). DIPEA (150 µL, 0.91 mmol) was added and the resulting mixture was stirred under argon at RT for 24 h. The coupling reaction was monitored by using TLC (chloroform/methanol 95:5). The solvent was removed under reduced pressure and the crude material was purified by column chromatography (3% MeOH/98% $CHCl_3$→5% MeOH/98% $CHCl_3$). The pure title compound was isolated as a purple solid (266 mg, 0.14 mmol, 32%). ^{1}H NMR (300 MHz, $CDCl_3$, 25°C): δ = 9.17 (brs, 2H; NHCOCH$_2$), 8.81 (d, J-(H,H) = 4.7 Hz, 4H; β-pyrrole CH), 8.67 (d, J(H,H) = 4.7 Hz, 4H; β-pyrrole CH), 8.62 (s, 8H; β-pyrrole CH), 8.16 (d, J(H,H) = 7.9 Hz, 4H; phenyl-H), 8.02 (d, J(H,H) = 7.9 Hz, 4H; phenyl-H), 7.27 (brs, 12H; mesityl CH), 7.14 (brs, 2H; NHCOCH$_2$), 3.62 (brs, 2H; NCH_2CC), 3.47 (m, 4H; CH_2NH), 2.84 (m, 4H; NCH_2CH$_2$), 2.71 (m, 4H; CH_2CO), 2.63 (s, 6H; 2× methyl CH_3), 2.61 (s, 12H; 4× methyl CH_3), 2.55 (m, 4H; CH_2CO), 2.34 (s, 1H; CCH), 2.26 (m, 4H; CH$_2$CH_2CH$_2$), 1.86 (s, 16H; 2× CH$_2$CH_2CH$_2$, 4× methyl CH_3), 1.84 (s, 24H; 8× methyl CH_3), −2.55 ppm (brs, 4H; NH); MS (MALDI-TOF): *m/z* calcd for $C_{125}H_{125}N_{13}O_4$: 1872.01; found: 1872.78 $[M]^{+\cdot}$.

Zinc G2 dendron (30): Compound **26** (266 mg, 0.14 mmol) was dissolved in $CHCl_3$ (10 mL). A saturated solution of zinc acetate in methanol (1 mL) was added and the solution was heated at reflux for 1 h. After the solvent was removed, the residue was taken up in CH_2Cl_2 (20 mL) and washed with water (2×20 mL). The organic layer was dried over $MgSO_4$. The crude product was purified by recrystallization from CH_2Cl_2/*n*-hexane to give the title compound as a purple solid (261 mg, 0.13 mmol, 92%). ^{1}H NMR (300 MHz, [D$_8$]THF, 25°C): δ = 9.79 (brs, 2H; NHCOCH$_2$), 8.80 (d, J(H,H) = 4.6 Hz, 4H; β-pyrrole CH), 8.61 (d, J-(H,H) = 4.6 Hz, 4H; β-pyrrole CH), 8.59 (s, 8H; β-pyrrole CH), 8.07 (brs, 8H; phenyl-H), 7.63 (m, 2H; NHCOCH$_2$), 7.27 (brs, 4H; mesityl CH), 7.25 (brs, 8H; mesityl CH), 3.45 (brs, 2H; NCH_2CC), 3.37 (m, 4H; CH_2NH), 2.59–2.46 (m, 27H; 2× NCH_2CH$_2$, 2× COCH_2, 2× methyl CH_3, 4× methyl CH_3, CCH), 2.44 (m, 4H; COCH_2), 2.17 (m, 4H; CH$_2$CH_2CH$_2$CO), 1.83 (s, 12H; 4× methyl CH_3), 1.82 (s, 24H; 8× methyl CH_3), 1.73 ppm (m, 4H; CH_2CH$_2$N); UV/Vis (CH_2Cl_2): λ_{max} ($\varepsilon\times10^{-3}$) = 421 (818), 550 (38.1), 589 nm (4.6 mol^{-1} L cm^{-1}); MS (MALDI-TOF): *m/z* calcd for $C_{125}H_{121}N_{13}O_4Zn_2$: 1995.82; found: 1995.79 $[M]^{+\cdot}$.

G3 dendron (27): Compound **24** (37.7 mg, 80.2 µmol) and the porphyrinic activated ester (**14**; 443 mg, 458 µmol) were dissolved in dry CH_2Cl_2 (13 mL). DIPEA (112 µL, 643 µmol) was added and the resulting mixture was stirred under argon at room temperature for 3 days. The solvent was removed under reduced pressure, and the crude material was purified by size-exclusion chromatographic (SEC) column (Bio-Rad Bio-Beads SX-1, CH_2Cl_2). The pure title compound was isolated as a purple solid (155 mg, 40.0 µmol, 50%). ^{1}H NMR (300 MHz, $CDCl_3$, 25°C): δ = 9.62 (brs, 4H; NHCOCH$_2$), 8.78 (d, J(H,H) = 4.6 Hz, 8H; β-pyrrole CH), 8.63 (d, J-(H,H) = 4.7 Hz, 8H; β-pyrrole CH), 8.59 (s, 16H; β-pyrrole CH), 8.12 (d, J(H,H) = 8.1 Hz, 8H; phenyl-H), 8.03 (d, J(H,H) = 8.1 Hz, 8H; phenyl-H), 7.40 (brs, 4H; NHCOCH$_2$), 7.24–7.17 (m, 24H; mesityl CH), 3.40 (m, 10H; NCH_2CC, 4× CH_2NH), 2.70–2.45 (m, 68H; 2× NCH_2CH$_2$, 2× CH$_2$CH_2N, 4× CH_2N, 4× CH_2CO, 4× methyl CH_3, 8× methyl CH_3, 4× CH_2CO), 2.24 (m, 9H; CH$_2$CH_2CH$_2$ and CCH), 1.83–1.77 (m, 84H; 2× CH$_2$CH_2CH$_2$, 4× CH$_2$CH_2CH$_2$, 8× methyl CH_3, 16× methyl CH_3), −2.58 ppm (brs, 8H; NH); UV/Vis (CH_2Cl_2): λ_{max} ($\varepsilon\times10^{-3}$) 419 (1472), 516 (68.5), 550 (26.9), 592 (20), 648 nm (13.8 mol^{-1} L cm^{-1}); MS (MALDI-TOF): *m/z* calcd for $C_{253}H_{260}N_{27}O_8$: 3804.08; found: 3804.09 $[M+H]^+$.

Zinc G3 dendron (31): Compound **27** (76.3 mg, 20.0 µmol) was dissolved in $CHCl_3$ (10 mL). A saturated solution of zinc acetate in methanol (1 mL) was added and the solution was heated at reflux for 1 h. After the

solvent was removed, the residue was taken up in CH_2Cl_2 (20 mL) and washed with water (2×20 mL). The organic layer was dried over $MgSO_4$. The crude material was purified by size-exclusion chromatographic (SEC) column (Bio-Rad Bio-Beads SX-1, CH_2Cl_2) and the pure title compound was isolated as a purple solid (64.9 mg, 16.0 μmol, 80%). ^{1}H NMR (300 MHz, [D$_8$]THF, 25°C): δ = 9.98 (brs, 4H; N*H*COCH$_2$), 8.58 (m, 8H; β-pyrrole C*H*), 8.56 (m, 24H; β-pyrrole C*H*), 8.11 (m, 8H; phenyl-*H*), 8.07 (m, 8H; phenyl-*H*), 7.87 (brs, 4H; N*H*COCH$_2$), 7.26–7.21 (m, 24H; mesityl C*H*), 3.44 (m, 10H; NCH_2CC, 4×CH_2NH), 2.66–2.41 (m, 69H; 2×NCH_2CH$_2$, 2×CH$_2$CH_2N, 4×CH_2N, 4×CH_2CO, 4× methyl CH_3, 8×methyl CH_3, 4×CH_2CO, CC*H*), 2.23 (m, 12H; 4× CH$_2$CH_2CH$_2$, 2×CH$_2$CH_2CH$_2$), 1.82–1.80 (m, 72H; 8×methyl CH_3, 16× methyl CH_3), 1.73 ppm (m, 8H; CH_2CH$_2$N); MS (MALDI-TOF): *m/z* calcd for $C_{253}H_{251}N_{27}O_8Zn_4$: 4059.51; found: 4059.04 $[M]^{+\bullet}$.

Zn$_4$G1 dendrimer (32): A mixture of zinc **G1** dendron **29** (26.8 mg, 27.6 μmol), zinc bisporphyrin **8** (19.1 mg, 13.8 μmol), copper(I) iodide (124.6 mg, 129 μmol), and DIPEA (43 μL, 260 μmol) in CH_2Cl_2 (5 mL) was stirred at RT for 24 h. The reaction mixture was washed with water (×2) and dried over anhydrous $MgSO_4$. The crude material was purified by repeated column chromatography (silica gel, $CHCl_3$→4% MeOH/96% $CHCl_3$) to give the pure title compound as a purple solid (24.2 mg, 7.3 μmol, 53%). ^{1}H NMR (300 MHz, [D$_8$]THF, 25°C): δ = 9.84 (brs, 2H; N*H*COCH$_2$), 9.04 (d, *J*(H,H) = 7 Hz, 2H; phenyl C*H*), 8.84 (d, *J*(H,H) = 4.5 Hz, 4H; β-pyrrole C*H*), 8.62 (d, *J*(H,H) = 4.5 Hz, 4H; β-pyrrole C*H*), 8.59 (s, 4H; β-pyrrole C*H*), 8.58 (s, 8H; β-pyrrole C*H*), 8.53 (d, *J*(H,H) = 4 Hz, 2H; β-pyrrole C*H*), 8.26 (brs, 2H; N*H*COCH$_2$), 8.20 (d, *J*(H,H) = 4 Hz, 2H; β-pyrrole C*H*), 8.17 (brs, 4H; *meso-H*), 8.13–8.04 (m, 10H; 8× phenyl C*H*, 2×phenyl C*H*), 8.01 (d, *J*(H,H) = 8 Hz, 2H; phenyl C*H*), 7.60 (m, 2H; phenyl C*H*), 7.39 (d, *J*(H,H) = 7 Hz, 2H; phenyl C*H*), 7.30 (t, *J*(H,H) = 7.6 Hz, 2H; phenyl C*H*), 7.27 (brs, 14H; mesityl C*H*, 2× NC*H*C), 7.00 (d, *J*(H,H) = 6.8 Hz, 2H; phenyl C*H*), 6.17 (brs, 4H CCH_2N), 4.82 (brs, 4H CCH_2NH), 3.45 (m, 4H; CH_2CH$_3$), 3.29 (m, 4H; CH_2CH$_3$), 2.71 (m, 4H; CH_2CH$_2$CH$_2$), 2.63–2.46 (m, 22H; 6×methyl CH_3, 2×CH$_2$CH$_2$CH_2), 2.37 (s, 12H; 4×methyl CH_3), 2.29 (m, 10H; 2× methyl CH_3, 2×CH$_2$CH_2CH$_2$), 1.83 (s, 12H; 4×methyl CH_3), 1.82 (s, 24H; 8×methyl CH_3), 1.33 ppm (t, *J*(H,H) = 7.7 Hz, 12H; 4×CH$_2$CH_3); MS (MALDI-TOF): *m/z* calcd for $C_{203}H_{178}N_{26}O_5Zn_4$: 3315.16; found: 3315.06 $[M]^{+\bullet}$.

Cu$_2$Zn$_2$G1 dendrimer (33): A mixture of zinc **G1** dendron **29** (30.1 mg, 31 μmol), free-base bisporphyrin **9** (19.5 mg, 15.5 μmol), copper(I) iodide (29.5 mg, 155 μmol), and DIPEA (51.4 μL, 311 μmol) in CH_2Cl_2 (6 mL) was stirred at RT for 48 h. The solution was concentrated under vacuum. The crude material was purified by repeated column chromatography (silica gel, $CHCl_3$→4% MeOH/96% $CHCl_3$) to give the pure title compound as a purple solid (13.5 mg, 4.1 μmol, 26%). UV/Vis (CH_2Cl_2): λ_{max} ($\varepsilon \times 10^{-3}$) = 394 (395), 420 (636), 549 nm (38.7 $mol^{-1}Lcm^{-1}$); MS (MALDI-TOF): *m/z* calcd for $C_{203}H_{181}Cu_2N_{26}O_5Zn_2$: 3320.19; found: 3320.20 $[M+H]^+$.

Cu$_2$Zn$_4$G2 dendrimer (34): A mixture of zinc **G2** dendron **30** (72.5 mg, 36.2 μmol), free-base bisporphyrin **9** (22.6 mg, 18.0 μmol), copper(I) iodide (42.6 mg, 224 μmol), and DIPEA (59.4 μL, 359 μmol) in CH_2Cl_2 (10 mL) was stirred at RT for 48 h. The reaction mixture was washed with water (×2) and dried over anhydrous $MgSO_4$. The crude material was purified by repeated size-exclusion chromatographic (SEC) column to give the pure title compound as a purple solid (46.4 mg, 8.6 μmol, 48%). MS (MALDI-TOF): *m/z* calcd for $C_{331}H_{310}Cu_2N_{40}O_9Zn_4$: 5382.08 (highest peak); found: 5382.18 $[M+H]^+$ (highest peak).

Cu$_2$Zn$_8$G3 dendrimer (35): A mixture of zinc **G3** dendron **31** (53.7 mg, 13.2 μmol), free-base bisporphyrin **9** (8.5 mg, 6.6 μmol), copper(I) iodide (14.5 mg, 224 μmol) and DIPEA (11.0 μL, 66.6 μmol) in CH_2Cl_2 (15 mL) was stirred at RT for 48 h. The reaction mixture was washed with water (×2) and dried over anhydrous $MgSO_4$. The crude material was purified by repeated size-exclusion chromatographic (SEC) column to give the pure title compound as a purple solid (46.2 mg, 4.9 μmol, 72%). MS (MALDI-TOF): *m/z* calcd for $C_{587}H_{570}Cu_2N_{68}O_{17}Zn_8$: 9499.08; found: 9499.46 $[M]^{+\bullet}$.

Acknowledgements

This research was supported by the Natural Sciences and Engineering Research Council of Canada (NSERC), le Fonds Québécois de la Recherche sur la Nature et les Technologies (FQRNT), and the Centre d'Études des Matériaux Optiques et Photoniques de l'Université de Sherbrooke, and l'Agence Nationale de la Recherche (ANR) is acknowledged for a Excellence Research Chair held in Dijon. The French Ministry of Research (MENRT), the CNRS (UMR 5260), and Région Bourgogne are also gratefully acknowledged. Dr Stéphane Brandès is gratefully acknowledged for recording the EPR spectra.

[1] a) M. Ayabe, A. Ikeda, Y. Kubo, M. Takeuchi, S. Shinkai, *Angew. Chem.* **2002**, *114*, 2914–2916; *Angew. Chem. Int. Ed.* **2002**, *41*, 2790–2792; b) S. Campidelli, C. Sooambar, E. Lozano Diz, C. Ehli, D. M. Guldi, M. Prato, *J. Am. Chem. Soc.* **2006**, *128*, 12544–12552; c) S. Cho, W.-S. Li, M.-C. Yoon, T. K. Ahn, D.-L. Jiang, J. Kim, T. Aida, D. Kim, *Chem. Eur. J.* **2006**, *12*, 7576–7584; d) M.-S. Choi, T. Aida, H. Luo, Y. Araki, O. Ito, *Angew. Chem.* **2003**, *115*, 4194–4197; *Angew. Chem. Int. Ed.* **2003**, *42*, 4060–4063; e) M.-S. Choi, T. Aida, T. Yamazaki, I. Yamazaki, *Chem. Eur. J.* **2002**, *8*, 2667–2678; f) T. Hasobe, P. V. Kamat, M. A. Absalom, Y. Kashiwagi, J. Sly, M. J. Crossley, K. Hosomizu, H. Imahori, S. Fukuzumi, *J. Phys. Chem. B* **2004**, *108*, 12865–12872; g) T. Hasobe, Y. Kashiwagi, M. A. Absalom, J. Sly, K. Hosomizu, M. J. Crossley, H. Imahori, P. V. Kamat, S. Fukuzumi, *Adv. Mater.* **2004**, *16*, 975–979; h) T. Hasobe, H. Murata, S. Fukuzumi, P. V. Kamat, *Mol. Cryst. Liq. Cryst.* **2007**, *471*, 39–51; i) C. F. Hogan, A. R. Harris, A. M. Bond, J. Sly, M. J. Crossley, *Phys. Chem. Chem. Phys.* **2006**, *8*, 2058–2065; j) M. Kozaki, A. Uetomo, S. Suzuki, K. Okada, *Org. Lett.* **2008**, *10*, 4477–4480; k) J. Larsen, J. Andersson, T. Polivka, J. Sly, M. J. Crossley, V. Sundstroem, E. Akesson, *Chem. Phys. Lett.* **2005**, *403*, 205–210; l) J. Larsen, B. Brueggemann, T. Khoury, J. Sly, M. J. Crossley, V. Sundstroem, E. Åkesson, *J. Phys. Chem. A* **2007**, *111*, 10589–10597; m) J. Larsen, B. Brueggemann, T. Polivka, V. Sundstroem, E. Aakesson, J. Sly, M. J. Crossley, *J. Phys. Chem. A* **2005**, *109*, 10654–10662; n) J. Larsen, B. Brueggemann, J. Sly, M. J. Crossley, V. Sundstroem, E. Aakesson, *Chem. Phys. Lett.* **2006**, *433*, 159–164; o) W. Maes, J. Vanderhaeghen, S. Smeets, C. V. Asokan, L. M. Van Renterghem, F. E. Du Prez, M. Smet, W. Dehaen, *J. Org. Chem.* **2006**, *71*, 2987–2994; p) J. B. Oh, M.-K. Nah, Y. H. Kim, M. S. Kang, J.-W. Ka, H. K. Kim, *Adv. Funct. Mater.* **2007**, *17*, 413–424; q) L. Valentini, M. Trentini, F. Mengoni, J. Alongi, I. Armentano, L. Ricco, A. Mariani, J. M. Kenny, *Diamond Relat. Mater.* **2007**, *16*, 658–663; r) J. Yang, S. Cho, H. Yoo, J. Park, W.-S. Li, T. Aida, D. Kim, *J. Phys. Chem. A* **2008**, *112*, 6869–6876; s) E. K. L. Yeow, K. P. Ghiggino, J. N. H. Reek, M. J. Crossley, A. W. Bosman, A. P. H. J. Schenning, E. W. Meijer, *J. Phys. Chem. B* **2000**, *104*, 2596–2606.

[2] W.-S. Li, T. Aida, *Chem. Rev.* **2009**, *109*, 6047–6076.

[3] P. D. Harvey, C. Stern, R. Guilard in *Handbook of Porphyrin Science, Vol. 11* (Eds.: K. Kadish, K. M. Smith, R. Guilard), World Scientific Publishing, Singapore, **2011**, 1–180.

[4] a) S. Faure, C. Stern, E. Espinosa, J. Douville, R. Guilard, P. D. Harvey, *Chem Eur. J.* **2005**, *11*, 3469–3481; b) S. Faure, C. Stern, R. Guilard, P. D. Harvey, *J. Am. Chem. Soc.* **2004**, *126*, 1253–1261.

[5] T. Förster, *Naturwissenschaften* **1946**, *33*, 166–175.

[6] a) C. J. Chang, Y. Deng, A. F. Heyduk, C. K. Chang, D. G. Nocera, *Inorg. Chem.* **2000**, *39*, 959–966; b) C. K. Chang, I. Abdalmuhdi, *J. Org. Chem.* **1983**, *48*, 5388–5390; c) C. K. Chang, I. Abdalmuhdi, *Angew. Chem.* **1984**, *96*, 154–155; *Angew. Chem. Int. Ed. Engl.* **1984**, *23*, 164–165; d) J. P. Collman, J. E. Hutchison, M. A. Lopez, A. Tabard, R. Guilard, W. K. Seok, J. A. Ibers, M. L'Her, *J. Am. Chem. Soc.* **1992**, *114*, 9869–9877; e) C. P. Gros, S. M. Aly, M. El Ojaimi, J.-M. Barbe, F. Brisach, A. S. Abd-El-Aziz, R. Guilard, P. D. Harvey, *J. Porphyrins Phthalocyanines* **2007**, *11*, 244–257; f) C. P. Gros, F. Brisach, A. Meristoudi, E. Espinosa, R. Guilard, P. D. Harvey, *Inorg. Chem.* **2007**, *46*, 125–135.

[7] L. Wen, M. Li, J. B. Schlenoff, *J. Am. Chem. Soc.* **1997**, *119*, 7726–7733.
[8] J.-M. Barbe, G. Canard, S. Bandès, R. Guilard, *Eur. J. Org. Chem.* **2005**, 4601–4611.
[9] L. Farrugia, *J. Appl. Crystallogr.* **1997**, *30*, 565.
[10] Y. Kobuke, *Struct. Bonding (Berlin)* **2006**, *121*, 49–104.
[11] I. V. Sazanovich, A. Balakumar, K. Muthukumaran, E. Hindin, C. Kirmaier, J. R. Diers, J. S. Lindsey, D. F. Bocian, D. Holten, *Inorg. Chem.* **2003**, *42*, 6616–6628.
[12] a) B. J. Littler, Y. Ciringh, J. S. Lindsey, *J. Org. Chem.* **1999**, *64*, 2864–2872; b) B. J. Littler, M. A. Miller, C.-H. Hung, R. W. Wagner, D. F. O'Shea, P. D. Boyle, J. S. Lindsey, *J. Org. Chem.* **1999**, *64*, 1391–1396.
[13] I. Maclnnes, J. C. Walton, *J. Chem. Soc. Perkin Trans. 2* **1987**, *64*, 1077–1082.
[14] a) J. P. André, C. F. G. C. Geraldes, J. A. Martins, A. E. Merbach, M. I. M. Prata, A. C. Santos, J. J. P. de Lima, E. Tóth, *Chem. Eur. J.* **2004**, *10*, 5804–5816; b) F. Dioury, I. Sylvestre, J.-M. Siaugue, V. Wintgens, C. Ferroud, A. Favre-Réguillon, J. Foos, A. Guy, *Eur. J. Org. Chem.* **2004**, 4424–4436.
[15] M. C. O'Sullivan, D. M. Dalrymple, *Tetrahedron Lett.* **1995**, *36*, 3451.
[16] G. Yao, K. Steliou, *Org. Lett.* **2002**, *4*, 485–488.
[17] a) V. V. Rostovtsev, L. G. Green, V. V. Fokin, K. B. Sharpless, *Angew. Chem.* **2002**, *114*, 2708–2711; *Angew. Chem. Int. Ed.* **2002**, *41*, 2596–2599; b) C. W. Tornøe, C. Christensen, M. Meldal, *J. Org. Chem.* **2002**, *67*, 3057–3064.
[18] M. Okada, Y. Kishibe, K. Ide, T. Takahashi, T. Hasegawa, *Int. J. Carbohydrate Chem.* **2009**, 305276.
[19] a) J.-S. Marois, K. Cantin, A. Desmarais, J.-F. Morin, *Org. Lett.* **2008**, *10*, 33–36; b) J.-S. Marois, J.-F. Morin, *Langmuir* **2008**, *24*, 10865–10873.
[20] a) S. L. Elmer, S. Man, S. C. Zimmerman, *Eur. J. Org. Chem.* **2008**, 3845–3851; b) S. Punidha, J. Sinha, A. Kumar, M. Ravikanth, *J. Org. Chem.* **2008**, *73*, 323–326.
[21] S. S. Eaton, G. R. Eaton, C. K. Chang, *J. Am. Chem. Soc.* **1985**, *107*, 3177–3184.
[22] C. J. Chang, E. A. Baker, B. J. Pistorio, Y. Deng, Z.-H. Loh, S. E. Miller, S. D. Carpenter, D. G. Nocera, *Inorg. Chem.* **2002**, *41*, 3102–3109.
[23] W. R. Scheidt, Y. J. Lee, *Struct. Bonding (Berlin)* **1987**, *64*, 1–70.
[24] D. Kim, D. Holten, M. Gouterman, *J. Am. Chem. Soc.* **1984**, *106*, 2793–2798.
[25] M. Pineiro, A. L. Carvalho, M. M. A. Pereira, A. M. Rocha Gonsalves, L. G. Arnaut, S. J. Formosinho, *Chem. Eur. J.* **1998**, *4*, 2299–2307.
[26] A. Harriman, *J. Chem. Soc. Faraday Trans. 1* **1981**, 77, 369–377.
[27] K. L. Cunningham, K. M. McNett, R. A. Pierce, K. A. Davis, H. H. Harris, D. M. Falck, D. R. McMillin, *Inorg. Chem.* **1997**, *36*, 608–613.
[28] E. I. Sagun, É. I. Zen'kevich, V. N. Knyukshto, A. Shul'ga, *M. Opt. Spectrosc.* **2005**, *99*, 731–743.
[29] a) I. V. Sazanovich, V. A. Ganzha, B. M. Dzhagarov, V. S. Chirvony, *Chem. Phys. Lett.* **2003**, *382*, 57–64; b) X. Yan, D. Holten, *J. Phys. Chem.* **1988**, *92*, 5982.
[30] S. G. Kruglik, P. A. Apanasevich, V. S. Chirvony, V. V. Kvach, V. A. Orlovich, *J. Phys. Chem.* **1995**, *99*, 2978–2995.
[31] S. G. Kruglik, V. V. Ermolenkov, A. G. Shvedko, V. A. Orlovich, V. A. Galievsky, V. S. Chirvony, C. Otto, P.-Y. Turpin, *Chem. Phys. Lett.* **1997**, *270*, 293–298.
[32] V. S. Chirvony, M. Négrerie, J.-L. Martin, P.-Y. Turpin, *J. Phys. Chem. A* **2002**, *106*, 5760–5767.
[33] a) M. Asano-Someda, T. Ichino, Y. Kaizu, *J. Phys. Chem. A* **1997**, *101*, 4484–4490; b) M. Asano-Someda, Y. Kaizu, *Inorg. Chem.* **1999**, *38*, 2303–2311; c) O. Ohno, Y. Ogasawara, M. Asano, Y. Kajii, Y. Kaizu, K. Obi, H. Kobayashi, *J. Phys. Chem.* **1987**, *91*, 4269–4273.
[34] N. Toyama, M. Asano-Someda, T. Ichino, Y. Kaizu, *J. Phys. Chem. A* **2000**, *104*, 4857–4865.
[35] A. Harriman, *J. Chem. Soc. Faraday Trans. 1* **1980**, *76*, 1978–1985.
[36] a) M. Hugerat, O. Levanon, E. L. Biczok, H. Linschitz, *Chem. Phys. Lett.* **1991**, *181*, 400–406; b) U. Rempel, R. Brunn, C. von Borczyskowski, M. Hugerat, *Proc. SPIE* **1993**, *1921*, 122–130.
[37] G. D. Egorova, V. N. Knyukshto, K. N. Solovev, M. P. Tsvirko, *Opt. Spektrosk.* **1980**, *48*, 1101.
[38] a) D. Bellows, S. M. Aly, C. P. Gros, M. El Ojaimi, J.-M. Barbe, R. Guilard, P. D. Harvey, *Inorg. Chem.* **2009**, *48*, 7613–7619; b) D. Bellows, T. Goudreault, S. M. Aly, D. Fortin, C. P. Gros, J.-M. Barbe, P. D. Harvey, *Organometallics* **2010**, *29*, 317–325.
[39] F. Bolze, C. P. Gros, M. Drouin, E. Espinosa, P. D. Harvey, R. Guilard, *J. Organomet. Chem.* **2002**, *643–644*, 89–97.
[40] A. Osuka, T. Nagata, F. Kobayashi, R. P. Zhang, K. Maruyama, N. Mataga, T. Asahi, T. Ohno, K. Nozaki, *Chem. Phys. Lett.* **1992**, *199*, 302–308.
[41] O. Gonen, H. Levanon, *J. Chem. Phys.* **1986**, *84*, 4132.
[42] a) A. C. Benniston, G. M. Chapman, A. Harriman, M. Mehrabi, *J. Phys. Chem. A* **2004**, *108*, 9026–9036; b) A. C. Benniston, A. Harriman, C. Pariani, C. A. Sams, *Phys. Chem. Chem. Phys.* **2006**, *8*, 2051–2057; c) P. K. Poddutoori, P. Poddutoori, B. G. Maiya, *J. Porphyrins Phthalocyanines* **2006**, *10*, 1049–1060; d) A. Prodi, M. T. Indelli, C. J. Kleverlaan, E. Alessio, F. Scandola, *Coord. Chem. Rev.* **2002**, *229*, 51–58; e) A. Prodi, C. J. Kleverlaan, M. T. Indelli, F. Scandola, E. Alessio, E. Iengo, *Inorg. Chem.* **2001**, *40*, 3498–3504; f) J. Seixas de Melo, A. J. F. N. Sobral, A. M. d. A. R. Gonsalves, H. D. Burrows, *J. Photochem. Photobiol. A* **2005**, *172*, 151–160.
[43] J. L. Sessler, B. Wang, A. Harriman, *J. Am. Chem. Soc.* **1995**, *117*, 704–714.
[44] Z. Otwinowski, W. Minor, *Methods Enzymol.* **1997**, *276*, 307.
[45] A. Altomare, M. C. Burla, M. Camalli, G. L. Cascarano, C. Giacovazzo, A. Guagliardi, A. G. G. Moliterni, G. Polidori, R. Spagna, *J. Appl. Crystallogr.* **1999**, *32*, 115–119.
[46] G. Sheldrick, *Acta Crystallogr. Sect. A* **2008**, *64*, 112–122.
[47] *SHELX-97*, Program for the Refinement of Crystal Structures, **1997**.
[48] U. Robben, I. Lindner, W. Gärtner, *J. Am. Chem. Soc.* **2008**, *130*, 11303–11311.

Received: June 15, 2011
Published online: November 14, 2011

